Carbohydrate Polymers 324 (2024) 121471

Contents lists available at ScienceDirect

Carbohydrate Polymers

journal homepage: www.elsevier.com/locate/carbpol

Smart fluorescent polysaccharides: Recent developments and applications

Diana C. Novo [a,b], Kevin J. Edgar [a,c,d,*]

[a] Department of Sustainable Biomaterials, Virginia Tech, Blacksburg, VA 24061, United States
[b] Department of Chemistry, Virginia Tech, Blacksburg, VA 24061, United States
[c] Macromolecules Innovation Institute, Virginia Tech, Blacksburg, VA 24061, United States
[d] GlycoMIP, National Science Foundation Materials Innovation Platform, United States

ARTICLE INFO

Keywords:
Fluorescence
Labeling
Bioavailability
Tracking
Amorphous solid dispersion
Drug delivery

ABSTRACT

Polysaccharides are ubiquitous, generally benign in nature, and compatible with many tissues in biomedical situations, making them appealing candidates for new materials such as therapeutic agents and sensors. Fluorescent labeling can create the ability to sensitively monitor distribution and transport of polysaccharide-based materials, which can for example further illuminate drug-delivery mechanisms and therefore improve design of delivery systems. Herein, we review fluorophore selection and ways of appending polysaccharides, utility of the product fluorescent polysaccharides as new smart materials, and their stimulus-responsive nature, with focus on their biomedical applications as environment-sensitive biosensors, imaging, and as molecular rulers. Further, we discuss the advantages and disadvantages of these methods, and future prospects for creation and use of these self-reporting materials.

1. Introduction

Low oral bioavailability is a crucial challenge to drug designers and formulators. Highly crystalline drugs are particularly problematic in this sense, as their lattice energy must be overcome for molecules of the solute to dissolve in the body (Teja et al., 2016). In addition to solubility issues, the drug must face several obstacles in the gastrointestinal (GI) tract (including chemical degradation in the acidic stomach) before absorption (primarily) through the epithelium of the small intestine. The amount of absorbed drug may be further reduced by other processes, such as metabolism by the liver and/or efflux transport (Collnot et al., 2007, 2010; Martinez & Amidon, 2002; Wempe et al., 2009). Drug-delivery systems (DDS) designed to dodge these obstacles are therefore in high demand.

Integration of functionally modified polysaccharides (PS) into DDS using amorphous solid dispersions (ASD) (Dong & Edgar, 2015; Ilevbare et al., 2013; Meng et al., 2014a; Mosquera-Giraldo et al., 2018; Novo et al., 2022; Wilson et al., 2018; Wilson et al., 2020), nanoparticles (Cheng et al., 2020; Gonzalez et al., 2022; G. Ricarte et al., 2019), or nanogels (Adav et al., 2010; Debele et al., 2016; Sun et al., 2018; Wang et al., 2020) has been reported to enhance drug solubility (Dong & Edgar, 2015; Liu, Taylor, & Edgar, 2015; Meng et al., 2014b; Teja et al., 2016). These DDS show promise for improving bioavailability (Chhatbar et al., 2011; Ilevbare et al., 2013) and controlled release of drugs and genetic material, including plasmid DNA, oligonucleotide, and signaling RNA (siRNA) (dos Santos & Grenha, 2015; Efiana et al., 2023; Fayazpour et al., 2006; Karimi Jabali et al., 2022; Messai et al., 2005; Samal et al., 2012; Weecharangsan et al., 2008). Being able to monitor these DDS using fluorescent probes can not only improve material design, but also can contribute to understanding how these drug-delivery systems work. Most polysaccharide derivatives used in DDS do not have strong chromophores. Natural PS typically do not possess UV absorbers, while the most typical alkanoate or alkyl substituents also do not absorb strongly in the UV (phthalate substituents being the only (somewhat) common exception). This absence of chromophores in PS makes them a challenge to detect spectroscopically, particularly in a diverse matrix of naturally occurring substances (including metabolites). Current methods for tracking PS include colorimetric (Englyst & Hudson, 1987; Janda & Work, 1971; Kohn & Wilchek, 1978; Lai et al., 2021), immunoassay (Mansur et al., 2014; Natarajan et al., 2021; Nualnoi et al., 2016; Salgado et al., 2021; Zhou et al., 2022), radioisotopic (Kaneo et al., 2001; Zheng et al., 2022) and fluorescent labeling strategies (Mary et al., 2022; Nawaz et al., 2021; Zheng et al., 2020), with the latter two being the most sensitive. While radiolabeling most minimally changes structure and properties of the molecule that one wants to track, fluorescent labeling is more convenient as it does not require the special licensing or

* Corresponding author at: Department of Sustainable Biomaterials, Virginia Tech, Blacksburg, VA 24061, United States
E-mail address: kjedgar@vt.edu (K.J. Edgar).

https://doi.org/10.1016/j.carbpol.2023.121471
Received 29 May 2023; Received in revised form 27 September 2023; Accepted 6 October 2023
Available online 8 October 2023

training necessary to run a radioactive facility, which is costly to create and maintain. This review will focus on recent developments in environment-sensitive and stimuli-responsive fluorescent PS used for metal ion detection (in nature, including in the human body) (Li et al., 2022), or in delivering and monitoring therapeutic cargo as observed via changes in polarity or pH. Herein, we provide a brief background on labeling technique and selection, properties, advantages, and caveats for these applications.

1.1. Fluorescent labeling technique

Fluorescent labeling is one of the most sensitive and selective spectroscopic techniques, able to detect even single molecules. Drug and drug delivery polymer concentrations in the human body can often be in the nanomolar range, so fluorescence sensitivity is of crucial importance for monitoring such dilute systems. Prior to de-excitation, fluorescent molecules stay in the excited singlet state (10^{9}- 10^{8} s) for a time greater than the time required for molecules to absorb light (10^{15} s). In contrast to the absorbing species, this timescale gives the fluorescing species greater sensitivity to its environment. Thus, several important types of events can be detected, including proton transfer, solvent cage relaxation, conformational change, and translational or rotational change (Cantor & Schimmel, 1980). This method is highly useful, describing the local environment of the probe via solvatochromic red/blue shift effects, intermolecular interactions between two Förster resonance energy transfer (FRET) pair molecules that are sensitive to the distance separating them (Behanna et al., 2007), and the location of the probe via spatial monitoring of fluorescent signals.

Solvatochromic labels are often the only method available to study membranes and lipid layers at a molecular level (Reichardt, 1994). Several fluorophores characteristically quench in polar/aqueous environments (i.e., bathochromic dyes), whereas quenching is suppressed in nonpolar/hydrophobic and/or rigid environments (Cantor & Schimmel, 1980). Hypsochromic dyes are those which quench in nonpolar solvents and increase emission intensity in polar environments.

FRET is an excited state, nonradiative energy transfer between a donor and acceptor pair via dipole-dipole coupling, which occurs when there is spectral overlap between the emission of a fluorophore (donor) and the absorption of another molecule (acceptor) (Förster, 1948). The energy transfer between the FRET pair (Fig. 1) results in fluorescence intensity increase for the acceptor and reduction for the donor (as well as reduced donor fluorescence lifetime). FRET is a powerful tool that can measure small changes in distance between two fluorescent donor and acceptor molecules since energy transfer efficiency, E, is inversely related to the donor- acceptor distance (r) to the sixth power (Eq. (1)) (Lakowicz, 2006b).

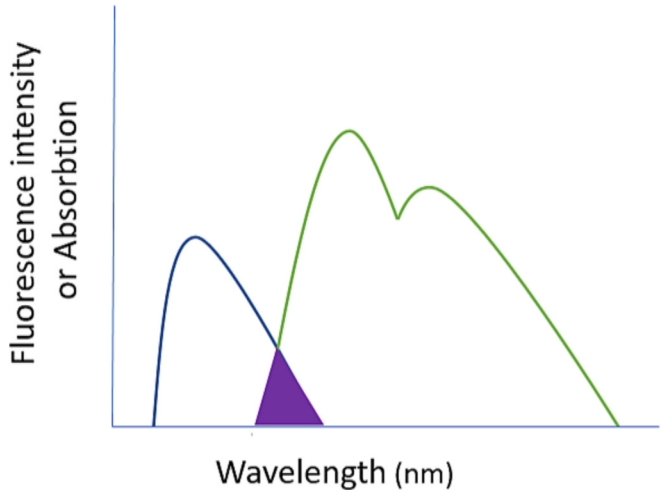

Fig. 1. FRET Spectral Overlap (Figure adapted from Lakowicz (2006a)). The excitation spectrum of the acceptor species (blue) in the absence of donor, and emission spectrum of the donor (green) in the absence of acceptor are depicted. The shaded region depicts the overlap integral between the two spectra. (For interpretation of the references to color in this figure legend, the reader is referred to the web version of this article.)

$$E = \frac{{}_0^6}{{}_0^6 + r^6} \quad (1)$$

A fluorescent polymer that forms a FRET pair with the drug permits measurement of the drug-polymer intermolecular distance for DDS (Ilevbare et al., 2013; Lakowicz, 2006a) since the R_0 term is in the range of biomacromolecule size (30–60 Å). FRET is highly useful as close proximity facilitates detection of drug-polymer interactions — believed to be a key element influencing drug crystallization and nucleation kinetics (Ilevbare et al., 2013). Thus, inhibition of drug crystallization can be confirmed with real-time fluorescent labeling techniques that reinforce comparative nucleation induction time data (Ilevbare et al., 2013). Furthermore, photobleaching experiments can establish whether changes in fluorescence are due to FRET phenomena. This is visualized by confocal microscopy by comparing pre- and post-photobleaching, indicating FRET with bleaching from the acceptor and recovery of emission via the donor chromophore (Behanna et al., 2007).

Fluorescence spectroscopy has become the gold standard for analysis of tagged biomolecules as fluorescence detection is highly sensitive, offering the ability to detect polymers containing low fluorophore loadings (degree of substitution (DS) = 0.05–0.001) with minimal depolymerization (de Belder & Wik, 1975). Multiple labels can be applied simultaneously if they do not spectrally overlap with FRET pairs, allowing high-throughput and automated instrumentation. Currently, radiolabeling methods only allow simultaneous analysis for up to two isotopes and require special instrumentation for analysis (e.g., dual channel detectors or imaging screens for isotopes (Belovolova & Glushkov, 2021), e.g., ^{3}H and ^{33}P). There are some potential disadvantages to fluorescent labeling compared to radiolabeling, such as toxicity, more significant structure modification, and spectral overlap with autofluorescent samples.

Several PS have been successfully fluorescently labeled and analyzed using UV-VIS, near-infrared (NIR) and fluorescence spectroscopic methods (Pereira, 2013; Wu et al., 2015), confocal laser scanning microscopy, fluorescent in situ hybridization, and flow cytometry (Adav et al., 2010; Behanna et al., 2007; Pramod et al., 2012). These methods can qualitatively identify tagged species and quantitatively map their biodistributions, biological mechanisms, intermolecular interactions, and thus, their roles in biologically significant events. This information lets one monitor the controlled release of drugs from delivery systems. This review aims to showcase the development of labeling techniques for PS derivatives, their selection, tagging methodologies, as well as their applications. It should be noted that all natural polysaccharides contain hydroxy groups, thus fluorescent labeling strategies that modify those groups will work on any polysaccharide. Strategies have also been developed to link fluorophores via polysaccharide carboxyls, i.e. the 6-carboxyl groups of uronic acids or introduced carboxyl-containing substituents like carboxymethyl groups. Amine groups (like the 2-amino-2-deoxy moieties of chitosan) may also be modified with fluorophores. Polysaccharides suitable for biomedical applications, including dextran, amylose, chitosan, and others, are quite frequently the subjects of fluorescent labeling studies.

1.2. Fluorophore selection

A fluorophore is a molecular entity that is excited by absorption of electromagnetic radiation of a certain wavelength, followed by re-emission of a lower energy photon that corresponds to a longer wavelength. Fluorophores can be classified as either intrinsic or extrinsic,

both of which possess conjugated π systems (polyaromatic hydrocarbons and/or heterocycles). Some common fluorophores are depicted in Fig. 2. Intrinsic fluorophores fluoresce in their native form, while extrinsic fluorophores fluoresce because an external fluorophore has been appended to them.

Intrinsic fluorophores found in nature include aromatic amino acid residues (Fig. 2A), flavins, and chlorophyll. Extrinsic fluorophores give fluorescence to compounds that lack the ability to fluoresce, or modify the sample's spectral properties if intrinsic fluorescence is inadequate or undesirable for the experimental design (Lakowicz, 2006a). The remainder of this review will focus on extrinsic fluorophores.

Ideal characteristics for a polysaccharide-linked fluorophore include a stable chemical linkage, high quantum yields and molar absorptivities, and the ability to operate at longer wavelengths - a safer range resulting in reduced sample photodecomposition compared to using high energy radiation (Adav et al., 2010). Ideal tags have excitation maxima accessible using simple light sources (laser diodes instead of LED) (Lakowicz, 2006a), chemical/photochemical stability, and readily accessible reactive groups to directly modify the PS of interest (Briggs et al., 1997). Should the polymer of interest contain an intrinsic fluorophore, the dye selected must possess a fluorescent profile which spectrally overlaps if desired for FRET measurements. Biological interferences caused by the tag's presence must be taken into account in order to consider its utility for the experimental objective. For example, the fluorophore could alter metabolism or transport in undesirable ways (Adav et al., 2010). The environment around the biomolecule of interest (i.e., its polarity or pH) can be probed with environment-sensitive fluorophores, divulging whether the molecule is in a hydrophobic or polar environment (Ilevbare et al., 2013; Lakowicz, 2006a). In order for any of these traits to be measurable, the fluorophore must be delivered and remain at its targeted destination long enough to be analyzed (Adav et al., 2010).

Fluorophores can be attached to biomolecules covalently, or through non-covalent associations via hydrophobic or electrostatic interactions (Lakowicz, 2006a; Webber, 1999). Modified fluorophores containing reactive electrophilic groups can undergo coupling to amines or undergo addition by nucleophiles to target macromolecules (Fig. 3A) (Adav et al., 2010; Waggoner, 1995), while those in Fig. 3B can react with thiols (Lakowicz, 2006a). Fluorescent alkyl halides can esterify carboxylic acid derivatives and react with thiols (Wiederschain, 2011). BODIPY 493/503 MeBr and 5-bromomethylfluorescein have the strongest fluorescence and absorptivities of any carboxyl derivative described to date (Wiederschain, 2011).

Dansyl groups offer sensitivity to polar solvents, long emission maxima (520 nm), and long fluorescence lifetimes, but have short wavelength absorption maxima (350 nm). Non-solvatochromic dyes that tend to self-quench include fluorescein, Rh, and BODIPY. Fluorescein and Rh are attractive labels as they are sensitive (indicated by their high molar extinction coefficients, 80,000 $\frac{M}{cm}$), have high quantum yields, and operate in long excitation (480 nm and 600 nm) and emission wavelength regions (510 and 615 nm), respectively (Lakowicz, 2006a). However, these dyes are being replaced with BODIPYs due to reduced self-quenching, higher quantum yields, and narrower emission spectra which permit greater resolution from other dyes (Lakowicz, 2006a). Unfortunately, BODIPYs have small Stokes shifts that can cause self-quenching from dye-dye energy transfers at sufficiently close Förster distances.

Although several environmental probes are available, the most well-studied is pyrene. Pyrene can probe structural changes, such as the concentration at which polymers begin to assemble or disassemble. The various microdomains of a nonlinear polymer chain, such as hydrophilic vs. hydrophobic, can begin to self-associate as a response to changes in the local environment. For example, changes in polarity or pH can lead to a shift in the concentration of hydrophobic domains, causing a shift in the emission spectrum of pyrene, specifically if there is an increase in the concentration of hydrophobic domains which begin to solubilize the probe. This point is defined as the critical aggregation concentration (CAC), critical micelle concentration (CMC), or critical vesicle concentration (CVC). Pyrene's characteristic emission spectrum provides values for the ratio of fluorescence intensities at 375 nm and 386 nm ($I_I/I_{III} = I_{375}/I_{386}$) for varying concentrations of sample. These ratios were plotted vs. log [polymer], and indicate the CVC at the instantaneous initial increase of of I_I/I_{III} (Belovolova et al., 2009; Pramod et al., 2012; Webber, 1999).

2. Applications

2.1. Toxic and heavy metal ion sensors

Decontaminating the environment is a critical global dilemma. Serious health concerns can emerge from organic and inorganic impurities that remain even after passage through a wastewater treatment plant, thereby reaching bodies of water and even downstream (to direct water consumers, to crops, and to other food sources). Chief sources of pollution from effluents include heavy metal ions and dyes from textile industries. Current decontamination methods such as hybrid ion exchange materials, activated carbon, or electrocoagulation are simply not always fully effective, or cost effective. Environmentally friendly, economical, and benign materials are thus highly attractive sources as antifoulants to remove heavy-metal toxins or dyes that are otherwise not degradable.

Chitosan is a randomly alternating linear polymer with β-(1 → 4) -linked D-glucosamine and *N*-acetyl-D-glucosamine units, derived from natural chitin found in crustacean exoskeletons by alkaline deacetylation. It is also found as a natural polymer in fungal cell walls (Abo Elsoud & El Kady, 2019). Chitosans have gained attention as abundant, renewable, and relatively nontoxic sources for an array of applications

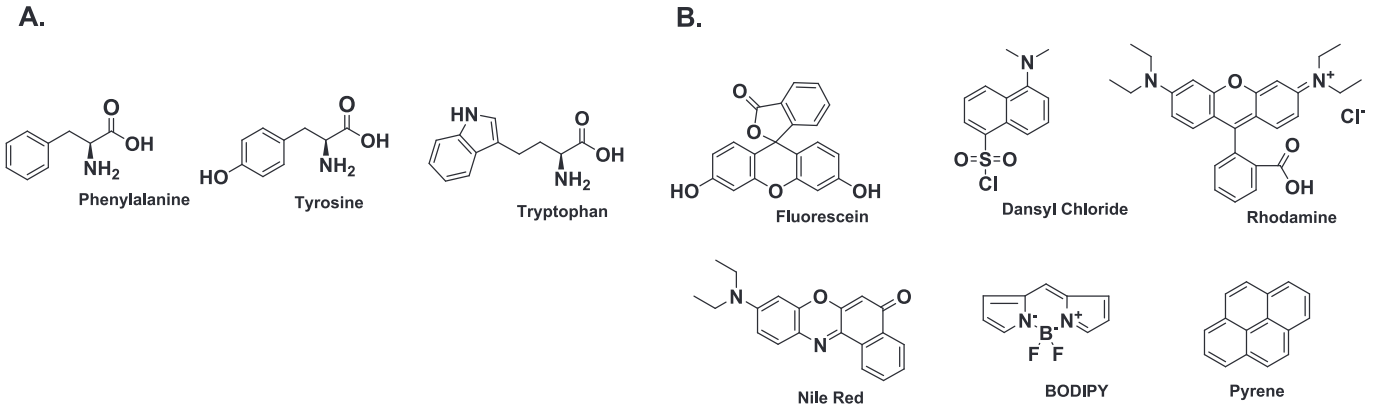

Fig. 2. Common fluorophores A. Intrinsic and B. Extrinsic.

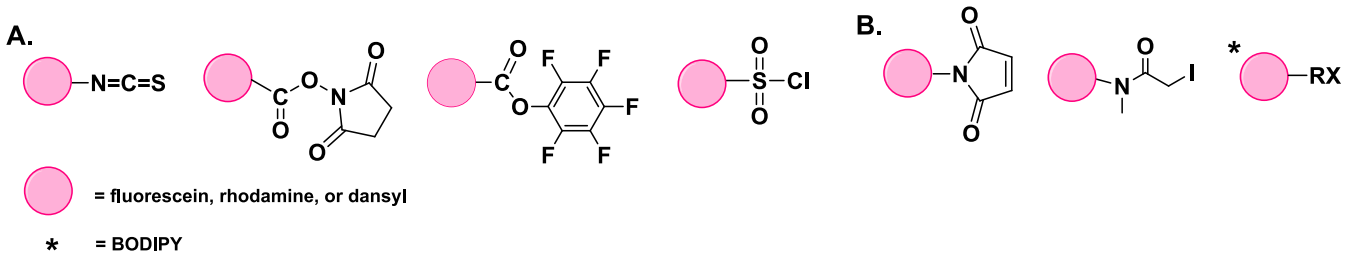

Fig. 3. Common Reactive Fluorophores. A. Isothiocyanates (ITC), succinimidyl (NHS) and pentafluorophenyl esters, and sulfonyl chlorides, B. Maleimide, Iodoacetamide, bromoacetamide, and alkyl halides (RX).

including in pesticides (Elsherbiny et al., 2022), paint coatings, biomedical products (wound dressings and antibacterial (Huang et al., 2019; Meng et al., 2010)), hydrogels, and as excellent metal ion (Gabris et al., 2022; Wan Ngah et al., 2011) and dye adsorbents (Pereira et al., 2017; Shahadat et al., 2022).

Chitosan has served as an eco-friendly clarifying agent with excellent chelating ability and high affinity for heavy metal ions including mercury (Bejan et al., 2020; Li et al., 2018), arsenic(V) (Gabris et al., 2022), chromium (Wani et al., 2021), copper (Li et al., 2020), and iron (Virmani et al., 2021). Chitosan's multifunctionality also permits binding to effluent dyes.

Recently, Bejan et al., 2018 synthesized a novel UV absorbing gel (xerogel) via Schiff-base chemistry linking the nontoxic formyl-phenothiazine and chitosan. Formyl-phenothiazine advantageously offers a strong green light emission profile with λ_{ex} at ~390 nm. The xerogel removes 15 environmentally threatening metals (Na^{+}, K^{+}, Ca^{2+}, Sr^{2+}, Ba^{2+}, Cr^{3+}, Mn^{2+}, Co^{2+}, Ni^{2+}, Cu^{2+}, Zn^{2+}, Cd^{2+}, Pb^{2+}, Eu^{3+}, Hg^{2+}) with high affinity and sensitivity to mercury (0.001 ppm) (Bejan et al., 2020). This porous xerogel displayed bathochromism, with a red shift when bound to mercury (yellow-green to green-yellow) along with changes in morphology to a rubber-like material. Swelling behavior was influenced by metal chelation, with an observed reduction for mass equilibrium swelling (20.8 when bound to just H, vs 11.8 for H—Ba).

Jia et al., 2018 prepared magnetic fluorescent nanoparticles with chitosan as a selective mercury (II) adsorbent with low detection limits of 12.43 nM. This recyclable system has chitosan as the shell, Fe_3O_4 nanoparticles as the core, and carbon dots (CDs) as the fluorescent probe, with only slight losses in adsorption (13 %) and photoluminescence (5 %) after recycling 5 times. This system has a well-defined structure with adsorption capacity of 110.52 mg/g, and quenches when Hg couples to the antifoulants as supported by the photoluminescence spectra.

Nanoaggregate polyelectrolytes of hyaluronic acid and/or chitosan complexes with luminescent lanthanide were recently designed to capture Eu^{3+} (Guo et al., 2018). The lanthanide-induced polysaccharide aggregates have employed either a single complex with one polyelectrolyte (polyanionic hyaluronic acid), or two oppositely charged polyelectrolytes (chitosan and hyaluronic acid). Fluorescence was significantly enhanced when using thenoyltrifluoroacetone (TTA) and 1,10-phenanthroline monohydrate (Phen) as ligands for Eu^{3+}.

A new fluorescent cotton fabric smart material with alginate-silver nanoparticles (AgNP) simultaneously detects bacteria (*Escherichia coli* and *Staphylococcus aureus*) while also removing transition metals (Na^{+}, K^{+}, Ca^{2+}, Cu^{2+}, and Zn^{2+}) that are toxic at elevated concentrations (Li et al., 2022). Silver nanoparticles are known to have antimicrobial properties, but are also toxic to humans and other organisms at higher concentrations. In contrast to an uncoated rare-earth complex, sodium alginate provided a supportive matrix for the stable, layer-by-layer formation of uniform sized nanoparticles (Nowak et al., 2021) with reduced toxicity confirmed by the cytochemical toxicity assay (MCC). Sodium alginate-AgNP and cotton were bonded via etherification with pentaerythritol. (Horrocks et al., 2005), and 3-chloro-2-hydroxypropyl trimethylammonium chloride enhanced binding between cotton and dye (Arivithamani & Giri Dev, 2017). Meanwhile, Eu^{3+}/TTA/Phen ligands induced nanoparticle assembly and enhanced fluorescence. This wearable fabric with relatively enhanced compatible technology allows straightforward evaluation by non-experts by exhibiting a strong red fluorescence that quenches when detecting increasing concentrations of toxin or metal. While unable to completely prevent the growth of bacteria, the smart fabric displayed antimicrobial activity by producing a 5 mm inhibition zone for *E. coli*, and 8 mm for *S. aureus*.

Water-soluble nitrogen-doped fluorescent CDs offer a straightforward and economical synthetic route to fluorescent materials with high performance, via one-pot carbonization of natural peach gum PS and ethylenediamine. This product offers enhanced quantum yields (23 % increase) vs. their undoped forms, low cytotoxicity, and fluorescence stability at various pH and ionic strength values, with rapid, selective, sensitive sensing of Au^{3+} ions. Au^{3+} sensing occurs via quenching effects, offering one of the lowest detection limits (6.4×10^{-8} M) in biological environments and river water. These traits make nitrogen-doped CDs promising, enhanced, and label-free alternatives for bioimaging and sensors (Liao et al., 2016).

2.2. *Enzyme/conjugate screening assays: localization and biological role determination*

An important advantage of fluorescent labeling is the ability to distinguish modified PS in the presence of endogenous PS (e.g. mannan, dextran, heparin, chondroitin sulfate, fucoidan). This approach permits localizing and quantifying cell surface proteins that bind to carbohydrates (lectins) (Adav et al., 2010; Glabe et al., 1983). Dextrans have been tagged with FITC and its *N*-fluoresceinyl thiocarbamate and fluoresceinyl triazine derivatives (Scheme 1A-B) to monitor cellular location of endosomes in kidneys (Lencer et al., 1990), blood-brain barrier permeability (Natarajan et al., 2017), gut barrier integrity (Gerkins et al., 2022), and controlled release (e.g. nasal (Ohtake et al., 2002) and dermal (Panda et al., 2022)). However, this FITC coupling strategy (Scheme 1) is not suitable for sulfated PS since conditions require solvolysis which promotes desulfation (Glabe et al., 1983). Stable linkages have been achieved with FITC-derivatized hyaluronic acids via isocyanate condensation, which can be extended to other carboxyl-containing PS (de Belder & Wik, 1975). Early fluorescein-PS derivatives (mannan, dextran, heparin, chondroitin sulfate and fucoidan) were prepared by Glabe et al. (1983) with minimally altered structure and therefore retention of structure-properties. This approach required pre-activation of the PS using cyanogen bromide (CNBr), followed by coupling with fluorescein amine (Scheme 1B). Effects of pH, incubation time, and equivalents of CNBr were found to impact the DS (Glabe et al., 1983).

The inhibiting activity of the resulting fluorescent PS was unaffected relative to underivatized PS (fucoidan, mannan, and heparin). Successes using this method include conservation of PS inhibiting activity for lectin-mediated hemagglutination and improved stability profiles (Glabe et al., 1983). The latter was determined by the absence of detectable free fluorescein post-incubation 3 months at 10 °C, 4 °C for 1 week, and for 2 days at 22 °C under alkaline conditions (up to pH 8) which are known to promote uncoupling. Product stability is postulated

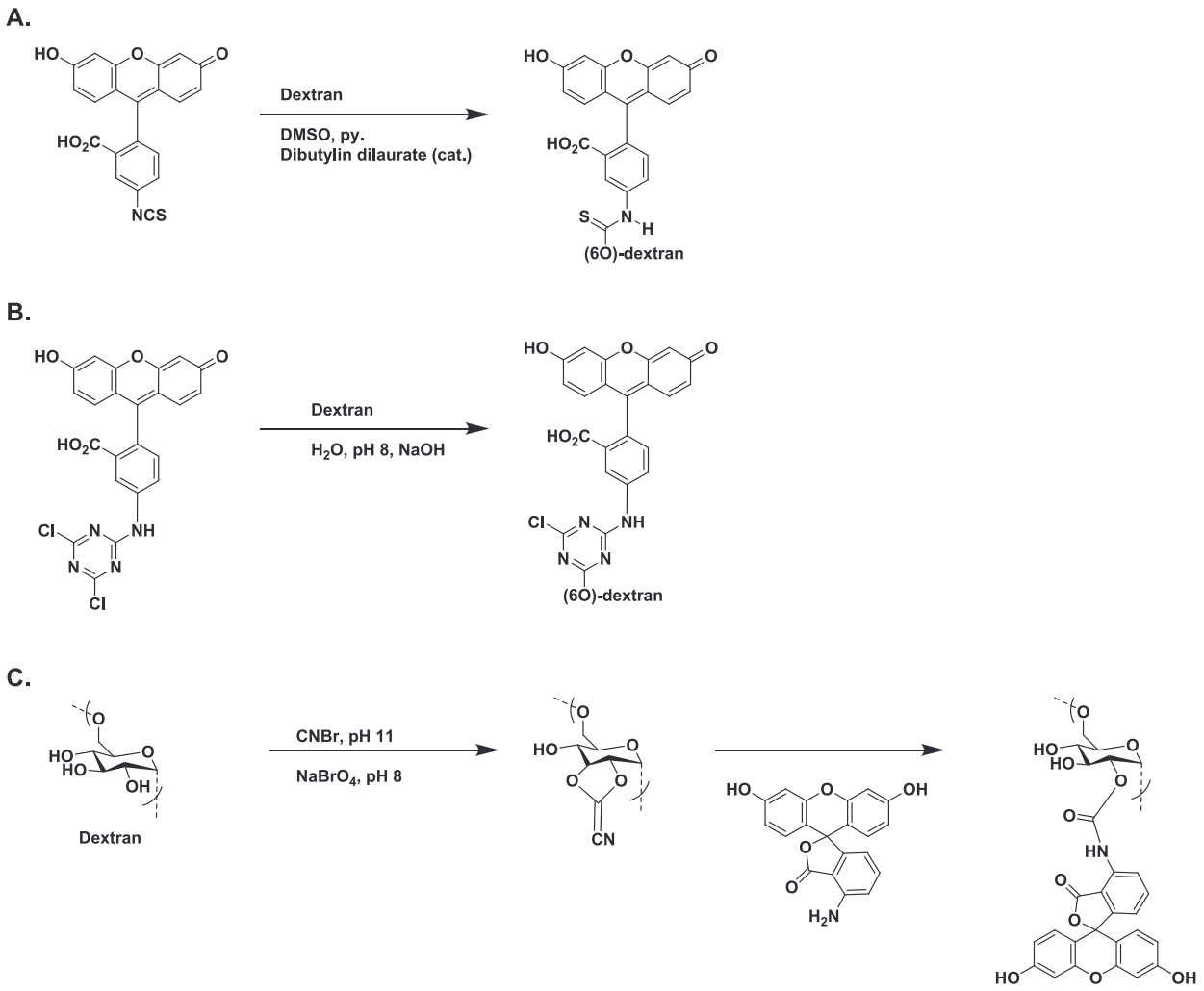

Scheme 1. Fluorescein-dextran tagging method: A) with FITC, B) with triazine derivative (de Belder & Wik, 1975), and C) activation of dextran with CNBr and coupled to fluoresceinamine (Glabe et al., 1983).

to result partially from lower p*K* values of fluoresceinamine's aromatic amine groups relative to those of previously studied saturated alkylamine groups. Retention of inhibitory activity from the lectin conjugates and site binding onto the cellular monolayer suggests their potential utility as cytochemical probes to study cell surface and PS interactions (Glabe et al., 1983).

Tags have been introduced to polymeric substances and *exo*-enzymes in bioaggregates to identify and quantify their significance in biological processes by generating aggregate distribution profiles (Adav et al., 2010). Localization and distribution of extracellular polymeric components were visualized by combining multiple color staining using fluorophores with confocal laser scanning microscopy, fluorescent in situ hybridization, and flow cytometry. Glycoconjugates of glycoproteins in bioaggregates have been stained using a FITC–labeled lectin, Concanavalin-A (Cerca et al., 2007; De Beer et al., 1996; Lawrence et al., 1998; Michael & Smith, 1995; Neu, 2000; Wang Yu Wang Yu Liu Joo-Hwa Tay, 2005). On/off quenching abilities of FITC-Concanavalin-A were discovered, as the FITC-Con-A-glycogen conjugate formation induces quenching (off), while dequenching (on) when disassembly is provoked by adding to the conjugate solution (Sato & Anzai, 2006). α-Mannopyranosyl and α-glucopyranosyl residues in bioaggregates have been stained with Con A-rhodamine conjugates (Adav et al., 2010; Chen, Lee, & Tay, 2007; Chen, Lee, Tay, & Show, 2007). Calcofluor White (CW), a fluorescence brightener, has been applied to β-linked PS for their identification and quantification in bioaggregates. CW staining techniques have characterized the distribution of three different PS in biofilms (Chen, Lee, & Tay, 2007). However, despite the high affinity of CW for cellulose and chitin, it may also interact with other PS (i.e., sialic acids, terminal glycan residues and lectins), creating the possibility of off-target results.

2.2.1. *Smart polysaccharides, molecular rulers*

Aggregation of co-assembled peptide amphiphile (PA) nanofibers (as donors) has been probed with commercial fluorescein-tagged heparin (the acceptor) (Behanna et al., 2007). This oppositely charged co-assembly consists of a bioactive heparin-selective binding epitope, and a non-bioactive stilbene tagged PA. The latter species can be viewed as an intrinsic fluorophore, as it contains branched stilbene. When the co-assembly contains a dilute chromophore component and is mixed with commercially tagged heparin, FRET indicates binding by increased fluorescein emission and quenched chromophoric PA emission. Specific vs. non-specific binding was confirmed, with ratio of acceptor to donor emission intensity plots for the PA pair containing an epitope and an epitope lacking PA pair control. Greater emissions were observed for the epitope-containing pair, indicating FRET events (as opposed to aggregate entanglement inducing spectral changes). Furthermore, FRET-induced fluorescent changes were confirmed by donor fluorescence recovery in photobleaching experiments. Thus, these epitope-containing probes can be used to sense and study PS interactions with other molecules (Behanna et al., 2007).

2.3. DDS, controlled release, and sensors

There are several routes available for drug administration including intravenous, inhalation, and transdermal, but the most patient-accepted route is oral administration. Development of high-performance DDS is motivated by the low bioavailability of many orally ingested drugs. Promising designs with enhanced fluorescence profiles for monitoring DDS, sensing, and controlled release have been observed in crosslinked non-nanoencapsulated systems and nanotherapeutics, including the naturally photoluminescent quantum dots.

2.3.1. Non-encapsulated DDS

A straightforward water-based method for amine grafting onto PS has been performed on the backbone of seaweed PS (including alginate, kappa-carrageenan, and agarose, Fig. 4) permitting observation of the influence of the amines on fluorogenic properties (Chhatbar et al., 2011; Oza et al., 2010; Oza, Meena, & Siddhanta, 2012; Oza, Prasad, & Siddhanta, 2012; Siddhanta et al., 2015). Since amides typically possess strong quenching abilities (Lukomska et al., 2001; Mrozek et al., 2005), it was surprising that fluorescent alginate-amide derivatives were afforded upon crosslinking (Chhatbar et al., 2011). This emerging fluorescence is thought to result from π-π* transitions from the newly introduced extended conjugated system when crosslinked with genipin (Chhatbar et al., 2011). This rapid and environmentally friendly method can be used even under neat conditions (Perreux et al., 2002).

Apart from the amide of alginate and ethylenediamine, other alginate – amide derivatives (hydrazine, ethylenediamine, hexanediamine and 1,4-cyclohexanediamine) exhibit fluorescence only after crosslinking with genipin (Scheme 2B). Increased fluorescence emissions were observed when the appended diamines had shorter oligo(methylene) spacers (Fig. 5A). Thus, alginate hydrazide was the most intensely fluorescent of this series when crosslinked with genipin, while the alginate amide with ethylenediamine fluoresced most intensely when not crosslinked (Chhatbar et al., 2011).

Crosslinked alginate derivatives containing the shortest difunctional amines studied, hydrazine and ethylenediamine, and higher DS (amide) produced the greatest emission intensities, producing an inverse correlation between the length of oligo(methylene) units and fluorescence emission (Fig. 5B) (Chhatbar et al., 2011). The observed weakened fluorescence for this crosslinked series as -CH_2- units increase is in agreement with diminished electron acceptor ability resulting from steric and inductive effects, caused by shortened spacer units (Braun et al., 1997). The dual fluorescence observed from alginate-ethylenediamine and the other crosslinked products (except alginate hydrazide) aligns with quenching induced via the torsion of the dimethylamino group with transfer of an electron (i.e., twisted intramolecular charge transfer (TICT) mechanism model), and nonradiative deactivation of the amide's n-π*transition energy states. Thus, amide acceptor ability can be tuned via alkyl group selection (Braun et al., 1997).

Labeled seaweed PS resulting from the grafting of nucleobases offer the ability to sense environments in biomedical applications (Scheme 3). Published examples include nucleobase modified agarose and kappa-carrageenan (Oza et al., 2010; Oza, Meena, & Siddhanta, 2012; Oza, Prasad, & Siddhanta, 2012).

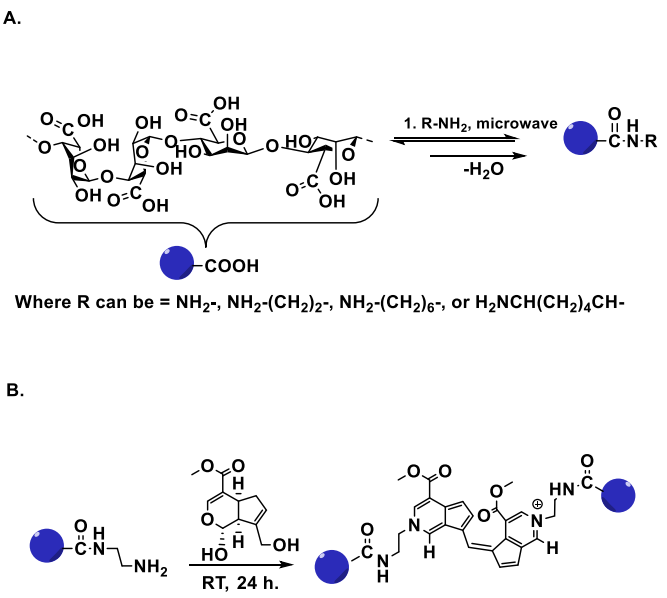

Scheme 2. A. Synthetic route for alginate amide derivatives B. Sample genipin crosslinking step for alginate-ethylenediamine derivative (Chhatbar et al., 2011).

These nucleobase-grafted PS were prepared using potassium persulfate as an initiator. When dye content is held at equal concentrations, the grafted products offered increased fluorescence intensities relative to the already fluorescent, free nucleobases (control). At the emission maximum, agarose grafted with guanine, cytosine, or adenine showed increased fluorescence intensity by 85 %, 143 %, and 30 % vs. agarose, respectively, while intensities of K-carrageenan grafted with adenine or cytosine increased by 40 % and 81 % vs. K-carrageenan itself, respectively. In contrast to guanine and cytosine, intensity enhancements from the grafted adenine analogs were similar when comparing to either controls at equal or higher dye content. Both cases produced greater emission intensities for agarose vs. K-carrageenan.

The fluorescence enhancement in solutions containing free dye at higher concentration relative to the grafted analogs can be attributed to diminished inter-nucleobase interactions (Oza et al., 2010; Oza, Meena, & Siddhanta, 2012; Oza, Prasad, & Siddhanta, 2012). This is because quenching likely occurs from stronger intermolecular interactions induced by greater concentrations (Callis, 1979), as was observed for higher concentrations of free nucleobase solutions. Reduced emission from adenine was attributed to the absence of a carbonyl group in contrast to guanine and cytosine, and π-π* transitions arising from adenine's increased nitrogen content. The former was unexpected since carbonyl-containing compounds typically quench in the presence of acidic proton sources and π-electron systems (Oza et al., 2010). Thus, greater emission from cytosine and guanine may be due to the carbonyl's rigid position which prevents internal proton transfers that would otherwise result in quenching (Oza, Meena, & Siddhanta, 2012). This effect is in agreement with reported emissions of grafted guanine and cytosine compared to the free dye at comparable concentrations, partly

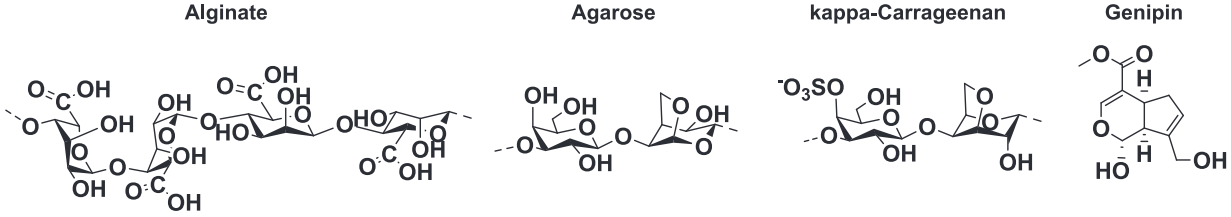

Fig. 4. PS used in microwave amidations employing the natural crosslinker genipin.

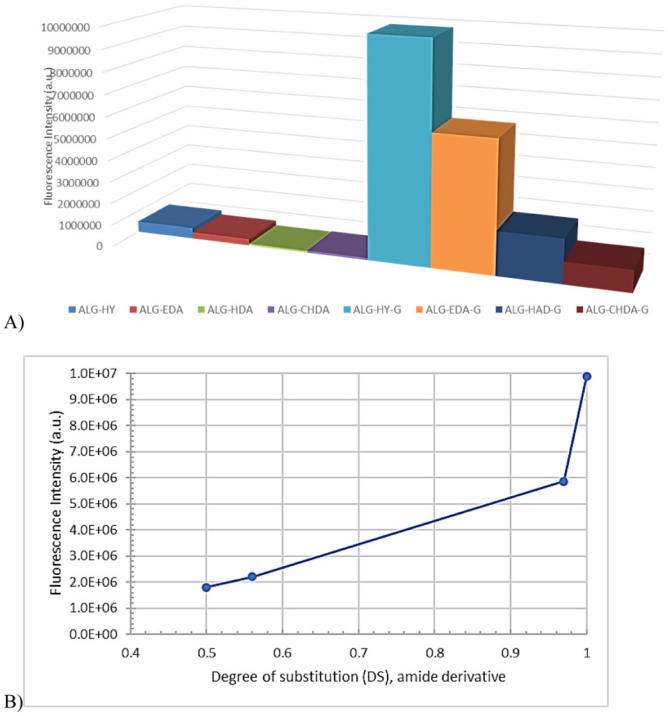

Fig. 5. (A) Fluorescence intensity of alginate (ALG) amide derivatives (hydrazine (HY), ethylenediamine (EDA), hexamethylenediamine (HDA), 1, 4-cyclohexanediamine (CHDA), and ALG amide-genipin crosslinked analogs (G)). (B) Fluorescence Intensity vs. DS of amide derivatives.
Figures adapted from Chhatbar et al. (2011) and Siddhanta et al. (2015).

from participation of fluorescence emissions from water and dilute aqueous media in PS-water matrices (Belovolova & Glushkov, 2021; Kondaveeti et al., 2014).

Other fluorescent labeling reactions of agarose are summarized in Scheme 4. Agarose has been linked with phthalimide to produce 6-deoxy-6-phthalimidoagarose, with subsequent removal of the phthaloyl protecting group by condensation with hydrazine hydrate. This method of introducing an accessible and protonated amine is promising for use in gene and drug delivery systems, creating the potential to derivatize 6-amino-6-deoxyagarose and other PS into polycationic polymers (Samal et al., 2012; Siddhanta et al., 2015). Fluorescence intensities of genipin-crosslinked 6-amino-6-deoxyagarose (produced similarly as shown in Scheme 2, B) with picolinic and nicotinic acid were increased vs. free picolinic and nicotinic acids (Kondaveeti et al., 2014).

Fluorescent labels have been introduced by esterification of agarose catalyzed by carbodiimides. Fluorescent agarose-L-tryptophan ester hydrogels synthesized using DCC/DMAP catalyst produced increased fluorescence emissions vs. free tryptophan. The corresponding crosslinked genipin hydrogels were stable under ambient conditions and over a wide pH range (Kondaveeti et al., 2013). Agarose has been esterified to append fluorescent 6-*O*-naphthylacetyl moieties using DCC/DMAP. This method shows promise as a sensor that controls release of the plant growth regulator, naphthyl acetic acid, in hydrolytic conditions (Kondaveeti et al., 2013).

2.3.2. *Nanotherapeutic systems*

Quercetin is a highly crystalline natural flavonoid which has been explored as a drug candidate. Both research studies and any clinical applications are impeded by its low bioavailability, caused in part by its poor water solubility (Gilley et al., 2017; Li et al., 2013). Zhou et al., 2022 employed a novel encapsulation structure with a low molecular weight chitosan nanoparticle composite as a DDS with the motivation to invoke antimicrobial properties, impart solubility, and thus enhance bioavailability. Chitosan formed uniform nanoparticles under acidic conditions; the nanoparticles were subsequently loaded with quercetin using sodium tripolyphosphate as crosslinker. The chitosan amine groups were then functionalized with FITC via EDC amide coupling to enable monitoring of antimicrobial properties towards *E. coli* using the Oxford cup method. The latter method is a standard test used to determine bacteriostatic properties, measured by how well the nanomaterial inhibits the spread of *E. coli* as determined by measuring colony diameter on a Petri dish. The further photoluminescence is observed from the sample spot, the less bacteriostatic is the material. Chitosan-quercetin drug-loaded nanoparticle spot diameter was equal to the inhibition zone, indicating highly successful antimicrobial performance. Chitosan-FITC nanoparticles have promise for tracking drug release and illuminating release mechanism.

Renewable polymersomes, which can load water-soluble or lipophilic drugs, were designed for cancer treatment using dextran, 3-pentadecylphenol, and tetraphenylethylene (TPE) (Virmani et al., 2021). This unique assembly manipulates FRET as a turn-off probe with the energy transfer between the aggregation induced emission polymersome host, TPE (donor), and encapsulated DOX (red luminescent acceptor) to detect breast cancer cells (MCF 7 cancer line). This phenomenon allows tracking DOX release kinetics, and for the first time, tracking the DDS within cells. Real-time enzymatic cleavage (esterase with higher cleavage efficiency vs. papain, trypsin, α-chymotrypsin, and glutathione) of the polymersome was observed with live-cell confocal microscopy by monitoring the restoration of the blue-luminescent signal as they 'turn-on', with DOX (in nucleus) and TPE (in lysosome) during endocytosis. Polymeric encapsulation was found to induce apopotosis to an extent equivalent to free DOX (80 %). Separately, cisplatin was conjugated to the polymersome and maintained blue luminescence while turning off during endocytosis. A cisplatin-loaded scaffold presented enhanced efficiency vs. free cisplatin, inducing apoptosis at 95 %.

Near infrared (NIR)-797 isothiocyanate (Fig. 6) has been used to label a bioreducible, disulfide-crosslinked heparin nanogel loaded with doxorubicin by conjugating ITC to heparin hydroxyl groups. Labeled heparin acts as a biomarker that can track the site and incidence of drug release monitored by in vivo real-time NIR fluorescent imaging and confocal microscopy. Tracking the fluorescent nanogel enables recording of time-dependent biodistributions as average % of injected dose/g wet tissue. This indicated long circulation times of the doxorubicin-loaded nanogel concentration in blood and effective targeting, since the nanogel concentration increased at the tumor site by two-fold within 24 h of injection (Wu et al., 2015).

NIR-797-heparin nanogels were incubated in fetal bovine serum (FBS) at 37 °C in order to evaluate NIR-797 physiological stability by UV–Vis spectroscopy. Stability was confirmed by the absence of released NIR-797 in FBS, thus NIR-797-heparin was deemed a viable tag for heparin nanogels. The disulfide bond is reduced in the intracellular environment, effectively eliminating crosslinks in the heparin nanogel and selectively releasing the encapsulated drug into the cytosol (Wu et al., 2015).

Hollow nanocapsules with aqueous cores prepared by cross-metathesis (CM) were created for targeting the water-oil interface using dextran acrylate and biodegradable unsaturated poly(phosphoester)s (PPEs). The therapeutic target is conveniently unaffected since the reaction occurs at the interface, producing stable microemulsions which form defined and discrete nanocapsules. Dextran acrylate was prepared in-house to control hydrophobicity, targeting DS (acrylate) of 0.13–0.55. Scheme 5 shows how one can target dye-tagging at either site of the nanocapsule: 2a) externally coupling onto the capsule's surface, or 2b) within the nanocapsule shell on the crosslinker's (PPE) pendent phosphoester. The latter uses a BODIPY derivative that simultaneously acts as a chain terminating agent during polycondensation as, unlike 2b, it lacks a terminal olefin (Malzahn et al., 2014).

Bonding between the nanocapsules and dye was confirmed using

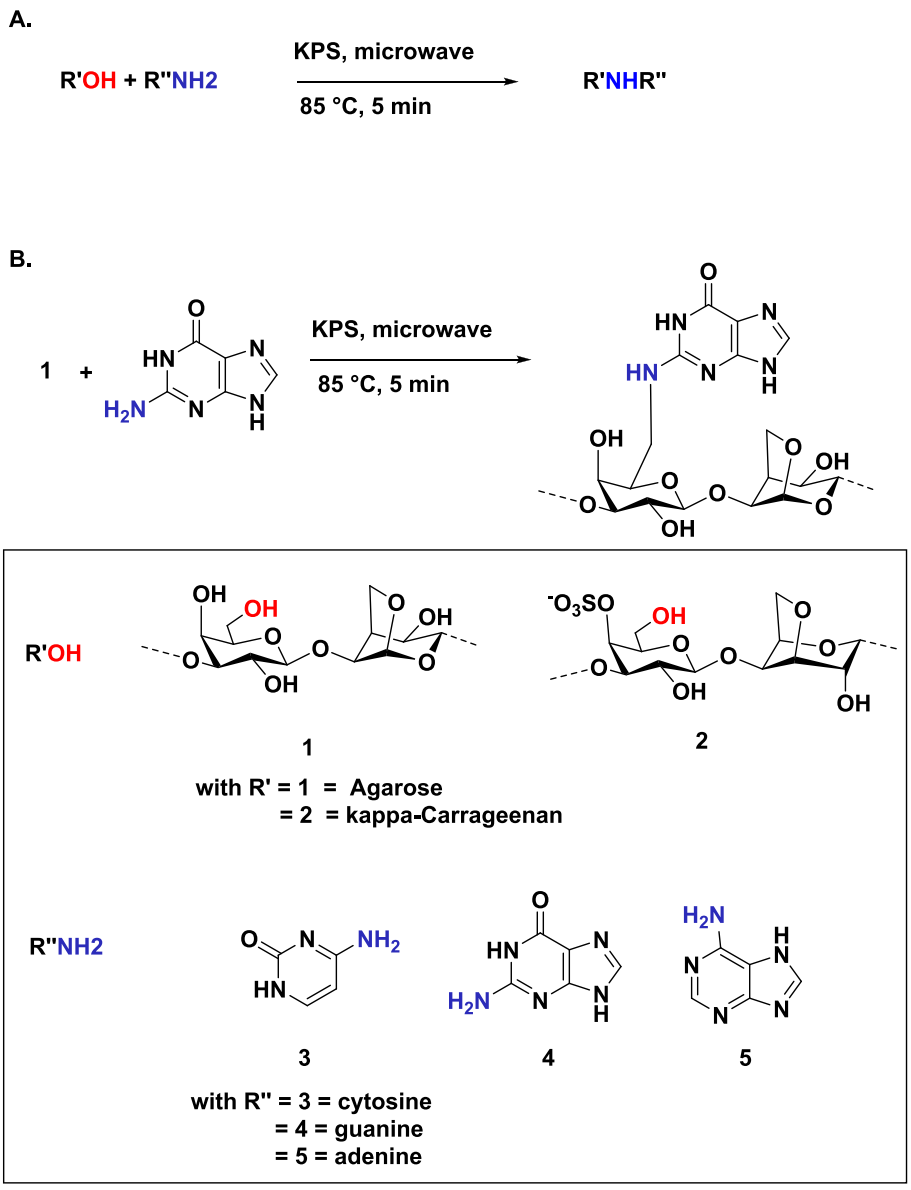

Scheme 3. General reaction scheme for nucleobase grafting onto agarose or kappa-carrageenan initiated by potassium persulfate (KPS) (top left), and a sample reaction (bottom left).

UV/VIS and fluorescence, and fluorescence correlation spectroscopy confirmed covalent bonding. The crosslinked product was initially inferred by its insolubility in all common solvents—possibly an undesirable trait for some drug-delivery applications. The versatility of this method is afforded through altering the olefin partners for CM either by using a different type of macromolecule for the type II olefin, or by varying the small molecule type I olefin. However, high conversion for CM has been reported for PS containing type I olefins tethered to type II olefin small molecules (Dong et al., 2016, 2017, 2019; Dong & Edgar, 2015; Meng et al., 2014b; Meng & Edgar, 2015; Novo et al., 2022). Promising applications of these biomolecule-loaded nanocapsules include targeted drug delivery and controlled release (Malzahn et al., 2014).

Amphiphilic dextran nanoscaffolds can selectively encapsulate hydrophilic and hydrophobic molecules for cellular drug delivery. This allows a PS-based vesicle to encapsulate either hydrophobic drugs in the shell, or water-soluble molecules in the core (Fig. 7) (Pramod et al., 2012).

This amphiphilic dextran derivative comprises a hydrophilic polymer backbone decorated with a hydrophobic tail (3-pentadecyl phenol (PDP), cardanol (CAR) or stearic acid (SA)), linked by an aliphatic ester. The amphiphilic character allows the polymer to assemble into vesicles in water or phosphate buffered saline via hydrophilic and hydrophobic interactions. The hydrophobic layer permits hydrophobic drug encapsulation, as its hydrophilic core can be loaded with hydrophilic drug. In physiological conditions, cytoplasmic esterase cleaves the ester linkage, resulting in rapid release of the encapsulated molecules. Molecules used in these loading experiments included the hydrophilic / water soluble Rhodamine-B and the hydrophobic polyaromatic anticancer drug, camptothecin (Pramod et al., 2012).

Rhodamine-B- and camptothecin-loaded vesicle uptake by mouse embryonic fibroblast cells was confirmed using confocal microscopy to produce fluorescence micrographs, demonstrating localization by comparing fluorescence intensity vs. cell location (Pramod et al., 2012). Dextran-PDP was able to deliver hydrophilic dye, Rh—B, as confirmed by its cellular uptake. The dye's strong emission profile also permitted direct visualization inside cells (Pramod et al., 2012). This methodology provides understanding of the endocytic cellular uptake mechanism and

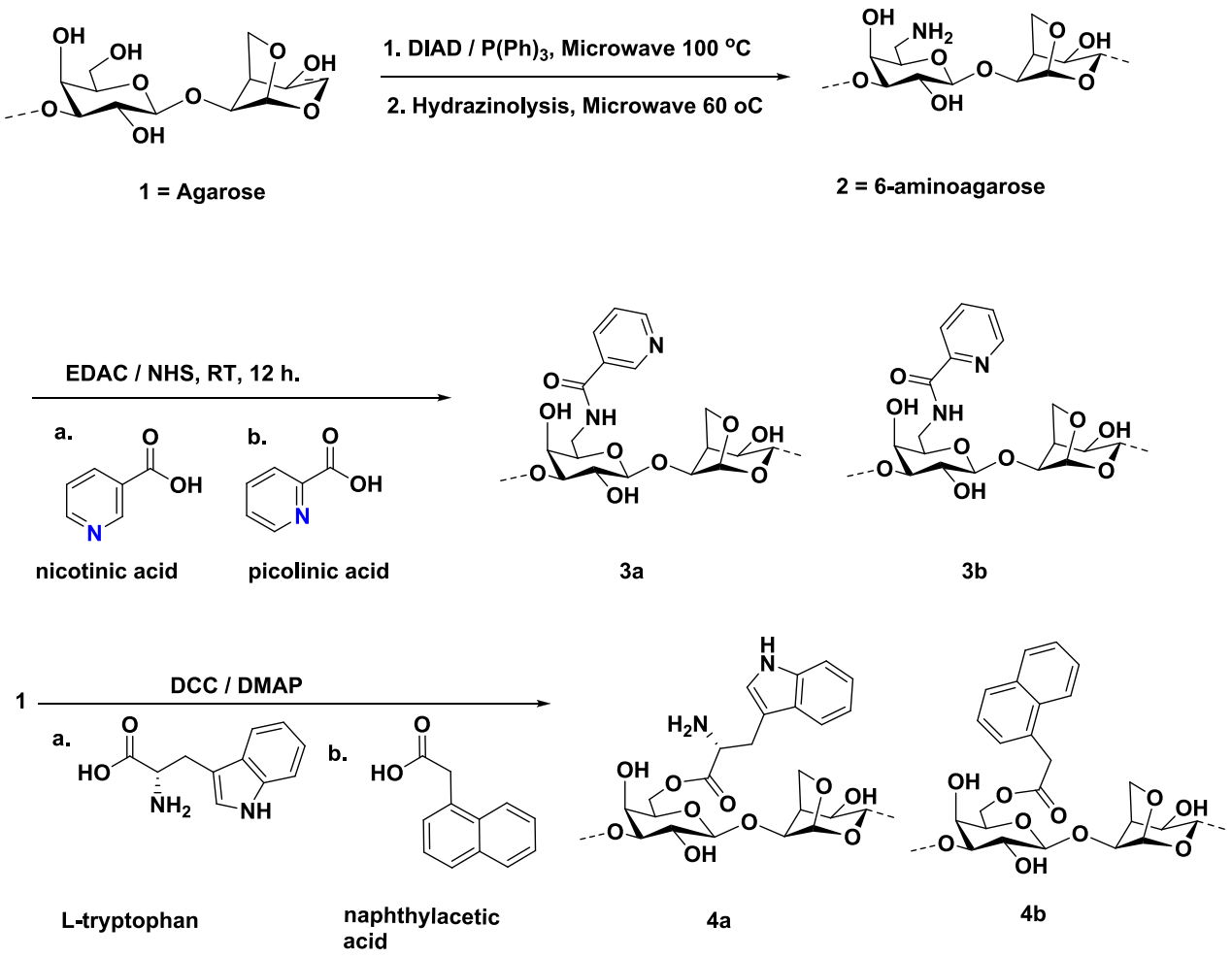

Scheme 4. Synthesis of 6-amino agarose (2), agarose amides: picolinic acid (3a), and nicotinic acid (3b), or agarose esters: L-tryptophan (4a), and 1-naphthylacetic acid (4b).

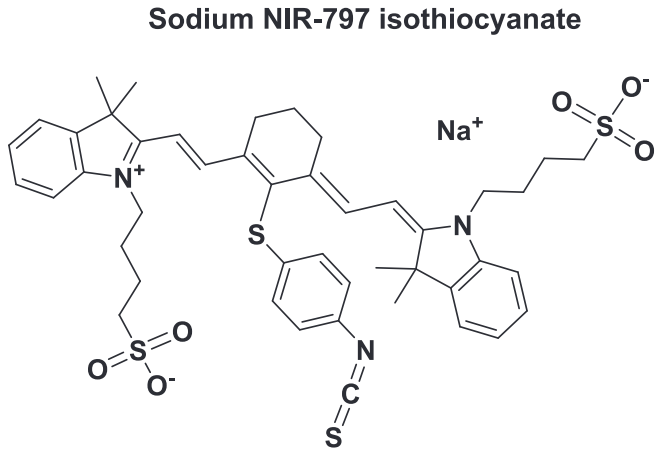

Fig. 6. NIR-797-isothiocyanate.

localization in healthy vs. cancer cells. The new and hydrolytically stable amphiphilic DDS design also allows simultaneous dual loading and delivery by encapsulation of both hydrophilic and hydrophobic drug molecules in a single nanoscaffold (Pramod et al., 2012). Stability against hydrolysis was enhanced by 10-fold for camptothecin-loaded polymer vs. free camptothecin which was confirmed by monitoring a red-shifted fluorescent absorbance relative to its non-encapsulated form in phosphate buffered saline.

2.3.3. Carbon dots (CDs)

Quantum dots are 1–10 nm, hydrophilic/polar materials, with adjustable particle size and high quantum yield, typically comprising C, Si, Se, or Cd (Zhou et al., 2018). CDs offer application opportunities across several fields, particularly in biolabeling and biosensing, as inherently luminescent materials. However, due to their high carbon content, several PS-CD tend to present low quantum yields and hydrophobicity in aqueous environments, thus making it desirable to enhance CD hydrophilicity (Ganguly et al., 2020; Richter et al., 2015).

Carboxymethyl chitosan quantum dots have been invented for lysozyme detection with high sensitivity (1.1–1.2 ng/mL). Zinc was found to reduce fluorescence detection limit to 0.031 ng/mL. This on-off sensor quenches as carboxymethyl chitosan is hydrolyzed upon the presence of lysozyme, triggering Zn^{2+} release while the quantum dots complex to lysozyme (Song et al., 2014). Quenching was observed with increasing temperature, reaction time, lower Zn^{2+} concentrations, and when decreasing in acidity in the range of pH 4–6.

Alginate nitrogen-doped CDs (urea) were thermally (microwave-induced) coupled via carbonization (Ganguly et al., 2020). EDAC-NHS was used to couple DOX onto alginate and explore in vitro release kinetics for controlled drug delivery. Enhanced solubility was observed as indicated by the transparent solution, imparted by the hydrophilicity of poly(anionic) alginate. Multiple labels can be employed with this material as it displays excitation dependence with a red shift in λ_{em} from 458 to 508 nm when increasing the λ_{ex} from 340 to 440 nm. The alginate

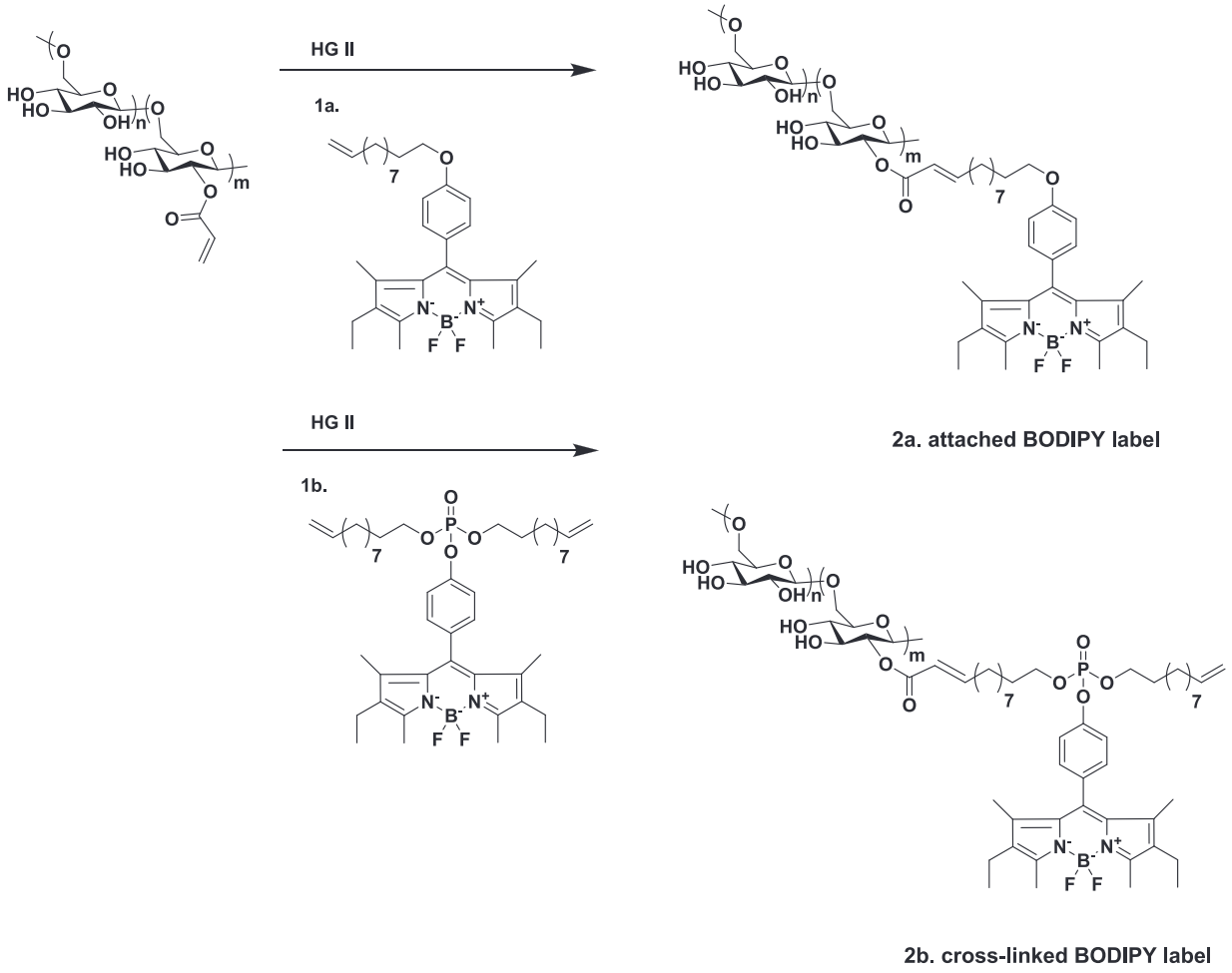

Scheme 5. CM of dextran acrylate using Hoveyda-Grubbs 2nd generation catalyst (HG II) to tag BODIPY onto 2a capsule's surface, or with 2b crosslinked phosphoester (Malzahn et al., 2014).

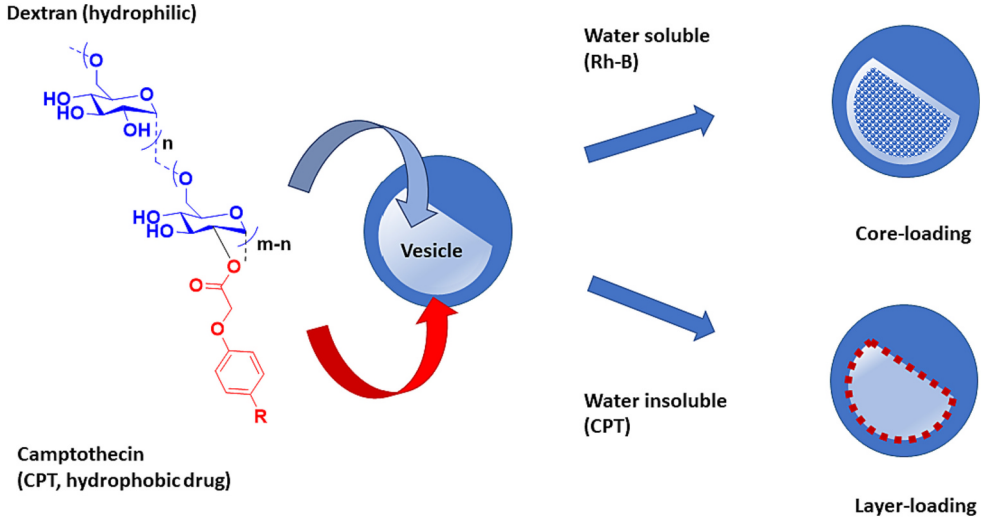

Fig. 7. Dextran vesicular delivery of hydrophobic or hydrophilic molecules. Figure adapted from Pramod et al. (2012).

urea carbon dot (AUCD) has blue fluorescence and 48 % quantum yield that is rather appreciable compared to other CDs (Table 1). The AUCD is stable in a range of conditions, displaying minimal change in fluorescence intensity after 3 months at room temperature, at 4–25 °C in the dark (9 months), and at different ionic strengths (0.25–2.5 M NaCl). The lifetime of these AUCD (2.90 ns) permits use in biological and electronic applications.

Table 1
Studies of different carbon dots comparing quantum yields with respect to alginate urea carbon dot (AUCD), adapted from Ganguly et al. (2020).

Precursor	Quantum yield (%)	Reference
Dopamine/cysteine	5.1	(Jana et al., 2016)
Polyethylene glycol (microwave)	16.0	(Jaiswal et al., 2011)
Polyethylene glycol (reflux)	45.1	(Kong et al., 2014)
Thioglycolic acid/CdCl	47.0	(Arivarasan et al., 2014)
Mannose/ammonium citrate	9.80	(Weng et al., 2015)
Anthracite/water	20.0	(Hu et al., 2016)
Glucosamine/water	16.8	(Liu, Zhao, et al., 2015)
L-glutamic acid	17.8	(Yu et al., 2016)
Alginate-urea	48.7	(Ganguly et al., 2020)

3. Conclusion

PS are important sustainable feedstocks as they are abundant, eco-friendly, often compatible with particular biological systems and circumstances, and are typically of low toxicity. The self-reporting abilities of smart fluorescent materials enable ease of detection with high specificity, selectivity, and sensitivity. Herein we highlight recent progress in stimulus-responsive labeled PS and how these promising biomaterials may be used to investigate and address emerging global challenges. PS-based carbon quantum dots are photoluminescent, high quantum yielding, economical materials for optical, environmental protection, bioimaging and biosensing applications. Chitosan, alginate, cellulose, heparin, and hyaluronic acid have served as important and efficient clarifying agents for the environment by removing toxic dyes and heavy metal toxic ions (in some cases, efficiently removing 15 metal ions at a time). PS-based labels have been employed to localize and determine the biological roles of enzymes or lectins, as well as in bioimaging, sensing, and theranostic applications to illuminate potential mechanisms including drug release kinetics in drug delivery systems and in animal trials. Several (still incurable) diseases, such as Alzheimer's, ulcerative colitis, or colorectal cancers remain poorly understood – recently, probes such as Dextran-FITC have shown great promise in deconvoluting how the gut microbiota are integral to several complex pathologies. We discussed effective approaches to append dyes onto PS with high conversion and fluorescence emissions with examples including cross-metathesis to probe drug loading, and facile coupling reactions with amides, esters, or protonated amines to decorate seaweed PS (alginate, kappa-carrageenan, and agarose) that have afforded highly fluorescent nucleobase or ester tagged materials that can be used in drug delivery or sensors. Use of newly developed turn-on/off probes such as polysaccharide-based smart fabrics or luminescent xerogels could be useful as straightforward, universal indicators to visually detect a broad array of hazards, including pathogens such as bacteria (*E. coli, Staphylococcus aureus*) or viruses, or heavy metal ions. The economical, eco-friendly, smart materials discussed hold promise for large scale reduction of toxic waste, containment of pathogens, as well as common day-to-day use across disciplines (food packaging (Dong et al., 2020) and anti-counterfeiting security (Liu et al., 2022; Peng et al., 2022; Wang et al., 2021; Zhang et al., 2023)). Despite these advances, fluoroprobe potential toxicity, physiological stability, and ability to be cleared from the human body are important issues that must be fully addressed in future research. We hope this review will stimulate further interest in and synthesis of efficient, novel, fluorescently-labeled PS with the ability to report environments of interest while remaining stable, and providing high Stokes shifts, large quantum yields, while effecting minimal destruction of the polymer structure and targeted properties.

CRediT authorship contribution statement

Diana C. Novo: Conceptualization, Methodology, Visualization, Writing – original draft, Writing – review & editing. **Kevin J. Edgar:** Conceptualization, Methodology, Visualization, Writing – original draft, Writing – review & editing.

Declaration of competing interest

The authors report no competing interests.

Data availability

No data was used for the research described in the article.

Acknowledgements

DN thanks the Department of Chemistry (VT) for partial support. Partial funding was also provided by the U.S. National Institutes of Health (R25GM072767; DN). We thank the U.S. National Science Foundation for partial support of this work through award number DMR-2204996. We would also like to thank Dr. Lynne Taylor, Dr. Chengzhe Gao, and Dr. Qingqing Qi for helpful discussions.

References

Abo Elsoud, M. M., & El Kady, E. M. (2019). Current trends in fungal biosynthesis of chitin and chitosan. *Bulletin of the National Research Centre, 43*(1), 1–12. https://doi.org/10.1186/S42269-019-0105-Y, 2019 43:1.

Adav, S. S., Lin, J. C. T., Yang, Z., Whiteley, C. G., Lee, D. J., Peng, X. F., & Zhang, Z. P. (2010). Stereological assessment of extracellular polymeric substances, exo-enzymes, and specific bacterial strains in bioaggregates using fluorescence experiments. In , *Vol. 28, Issue 2. Biotechnology advances* (pp. 255–280). Elsevier. https://doi.org/10.1016/j.biotechadv.2009.08.006.

Arivarasan, A., Sasikala, G., & Jayavel, R. (2014). In situ synthesis of CdTe:CdS quantum dot nanocomposites for photovoltaic applications. *Materials Science in Semiconductor Processing, 25*, 238–243. https://doi.org/10.1016/J.MSSP.2013.12.018

Arivithamani, N., & Giri Dev, V. R. (2017). Sustainable bulk scale cationization of cotton hosiery fabrics for salt-free reactive dyeing process. *Journal of Cleaner Production, 149*, 1188–1199. https://doi.org/10.1016/J.JCLEPRO.2017.02.162

Behanna, H. A., Rajangam, K., & Stupp, S. I. (2007). Modulation of fluorescence through coassembly of molecules in organic nanostructures. *Journal of the American Chemical Society, 129*(2), 321–327. https://doi.org/10.1021/JA062415B/SUPPL_FILE/JA062415BSI20060801_123301.PDF

Bejan, A., Ailincai, D., Simionescu, B. C., & Marin, L. (2018). Chitosan hydrogelation with a phenothiazine based aldehyde: A synthetic approach toward highly luminescent biomaterials. *Polymer Chemistry, 9*(18), 2359–2369. https://doi.org/10.1039/c7py01678f

Bejan, A., Doroftei, F., Cheng, X., & Marin, L. (2020). Phenothiazine-chitosan based eco-adsorbents: A special design for mercury removal and fast naked eye detection. *International Journal of Biological Macromolecules, 162*, 1839–1848. https://doi.org/10.1016/j.ijbiomac.2020.07.232

Belovolova, L. V., & Glushkov, M. V. (2021). Porous matrices and specific features of water in nanostructures. *Physics of Wave Phenomena, 29*(3), 249–277. https://doi.org/10.3103/S1541308X21030031, 2021 29:3.

Belovolova, L. V., Glushkov, M. V., Vinogradov, E. A., Babintsev, V. A., & Golovanov, V. I. (2009). Ultraviolet fluorescence of water and highly diluted aqueous media. *Physics of Wave Phenomena, 17*(1), 21–31. https://doi.org/10.3103/S1541308X0901004X

Braun, D., Rettig, W., Delmond, S., Letard, J. F., & Lapouyade, R. (1997). Amide derivatives of DMABN: A new class of dual fluorescent compounds. *Journal of Physical Chemistry A, 101*(37), 6836–6841. https://doi.org/10.1021/jp970168f

Briggs, M. S. J., Bruce, I., Miller, J. N., Moody, C. J., Simmonds, A. C., & Swann, E. (1997). Synthesis of functionalised fluorescent dyes and their coupling to amines and amino acids. *Journal of the Chemical Society, Perkin Transactions, 1*.

Callis, P. R. (1979). Polarized fluorescence and estimated lifetimes of the DNA bases at room temperature. *Chemical Physics Letters, 61*(3), 568–570. https://doi.org/10.1016/0009-2614(79)87174-2

Cantor, C. R., & Schimmel, P. R. (1980). *Biophysical chemistry: Part II: Techniques for the study of biological structure and function*. Macmillan.

Cerca, N., Oliveira, R., & Azeredo, J. (2007). Susceptibility of Staphylococcus epidermidis planktonic cells and biofilms to the lytic action of staphylococcus bacteriophage K. *Letters in Applied Microbiology, 45*(3), 313–317. https://doi.org/10.1111/J.1472-765X.2007.02190.X

Chen, M. Y., Lee, D. J., & Tay, J. H. (2007). Distribution of extracellular polymeric substances in aerobic granules. *Applied Microbiology and Biotechnology, 73*(6), 1463–1469. https://doi.org/10.1007/s00253-006-0617-x

Chen, M. Y., Lee, D. J., Tay, J. H., & Show, K. Y. (2007). Staining of extracellular polymeric substances and cells in bioaggregates. *Applied Microbiology and Biotechnology, 75*(2), 467–474. https://doi.org/10.1007/s00253-006-0816-5

Cheng, Q., Qin, W., Yu, Y., Li, G., Wu, J., & Zhuo, L. (2020). Preparation and characterization of PEG-PLA Genistein micelles using a modified emulsion-evaporation method. *Journal of Nanomaterials, 2020*, 1–15. https://doi.org/10.1155/2020/3278098

Chhatbar, M. U., Meena, R., Prasad, K., Chejara, D. R., & Siddhanta, A. K. (2011). Microwave-induced facile synthesis of water-soluble fluorogenic alginic acid derivatives. *Carbohydrate Research, 346*(5), 527–533. https://doi.org/10.1016/j.carres.2011.01.002

Collnot, E.-M., Baldes, C., Schaefer, U. F., Edgar, K. J., Wempe, M. F., & Lehr, C.-M. (2010). Vitamin E TPGS P-glycoprotein inhibition mechanism: Influence on conformational flexibility, intracellular ATP levels, and role of time and site of access. *Molecular Pharmaceutics, 7*(3), 642–651. https://doi.org/10.1021/mp900191s

Collnot, E.-M., Baldes, C., Wempe, M. F., Kappl, R., Hüttermann, J., Hyatt, J. A., … Lehr, C.-M. (2007). Mechanism of inhibition of P-glycoprotein mediated efflux by vitamin E TPGS: Influence on ATPase activity and membrane fluidity. *Molecular Pharmaceutics, 4*(3), 465–474. https://doi.org/10.1021/mp060121r

De Beer, D., O'Flaharty, V., Thaveesri, J., Lens, P., & Verstraete, W. (1996). Distribution of extracellular polysaccharides and flotation of anaerobic sludge. *Applied Microbiology and Biotechnology, 46*(2), 197–201. https://doi.org/10.1007/s002530050805

de Belder, A. N., & Wik, K. O. (1975). Preparation and properties of fluorescein-labelled hyaluronate. *Carbohydrate Research, 44*(2), 251–257. https://doi.org/10.1016/S0008-6215(00)84168-3

Debele, T. A., Mekuria, S. L., & Tsai, H. C. (2016). Polysaccharide based nanogels in the drug delivery system: Application as the carrier of pharmaceutical agents. In *, Vol. 68. Materials science and engineering C* (pp. 964–981). Elsevier Ltd.. https://doi.org/10.1016/j.msec.2016.05.121

Dong, H., Ling, Z., Zhang, X., Zhang, X., Ramaswamy, S., & Xu, F. (2020). Smart colorimetric sensing films with high mechanical strength and hydrophobic properties for visual monitoring of shrimp and pork freshness. *Sensors and Actuators, B: Chemical, 309*, Article 127752. https://doi.org/10.1016/j.snb.2020.127752

Dong, Y., & Edgar, K. J. (2015). Imparting functional variety to cellulose ethers via olefin cross-metathesis. *Polymer Chemistry, 6*(20), 3816–3827. https://doi.org/10.1039/C5PY00369E

Dong, Y., Mosquera-Giraldo, L. I., Taylor, L. S., & Edgar, K. J. (2016). Amphiphilic cellulose ethers designed for amorphous solid dispersion via olefin cross-metathesis. *Biomacromolecules, 17*(2), 454–465. https://doi.org/10.1021/acs.biomac.5b01336

Dong, Y., Mosquera-Giraldo, L. I., Taylor, L. S., & Edgar, K. J. (2017). Tandem modification of amphiphilic cellulose ethers for amorphous solid dispersion via olefin cross-metathesis and thiol-Michael addition. *Polymer Chemistry, 8*(20), 3129–3139. https://doi.org/10.1039/C7PY00228A

Dong, Y., Novo, D. C., Mosquera-Giraldo, L. I., Taylor, L. S., & Edgar, K. J. (2019). Conjugation of bile esters to cellulose by olefin cross-metathesis: A strategy for accessing complex polysaccharide structures. *Carbohydrate Polymers, 221*, 37–47. https://doi.org/10.1016/j.carbpol.2019.05.061

dos Santos, M. A., & Grenha, A. (2015). Polysaccharide nanoparticles for protein and peptide delivery: Exploring less-known materials. In *, Vol. 98. Advances in protein chemistry and structural biology* (pp. 223–261). Academic Press. https://doi.org/10.1016/bs.apcsb.2014.11.003.

Efiana, N. A., Kali, G., Fürst, A., Dizdarevic, A., & Bernkop-Schnürch, A. (2023). Betaine-modified hydroxyethyl cellulose (HEC): A biodegradable mucoadhesive polysaccharide exhibiting quaternary ammonium substructures. *European Journal of Pharmaceutical Sciences, 180*. https://doi.org/10.1016/j.ejps.2022.106313

Elsherbiny, A. S., Galal, A., Ghoneem, K. M., & Salahuddin, N. A. (2022). Novel chitosan-based nanocomposites as ecofriendly pesticide carriers: Synthesis, root rot inhibition and growth management of tomato plants. *Carbohydrate Polymers, 282*. https://doi.org/10.1016/J.CARBPOL.2022.119111

Englyst, H. N., & Hudson, G. J. (1987). Colorimetric method for routine measurement of dietary fibre as non-starch polysaccharides. A comparison with gas-liquid chromatography. *Food Chemistry, 24*(1), 63–76. https://doi.org/10.1016/0308-8146(87)90084-7

Fayazpour, F., Lucas, B., Alvarez-Lorenzo, C., Sanders, N. N., Demeester, J., & De Smedt, S. C. (2006). Physicochemical and transfection properties of cationic hydroxyethylcellulose/DNA nanoparticles. *Biomacromolecules, 7*(10), 2856–2862. https://doi.org/10.1021/bm060474b

Förster, T. (1948). Zwischenmolekulare energiewanderung und fluoreszenz. *Annalen der Physik, 437*(1–2), 55–75.

G. Ricarte, R., J. Van Zee, N., Li, Z., M. Johnson, L., P. Lodge, T., & A. Hillmyer, M. (2019). Recent advances in understanding the Micro- and nanoscale phenomena of amorphous solid dispersions. *Molecular Pharmaceutics, 16*(10), 4089–4103. https://doi.org/10.1021/acs.molpharmaceut.9b00601

Gabris, M. A., Rezania, S., Rafieizonooz, M., Khankhaje, E., Devanesan, S., AlSalhi, M. S., … Shadravan, A. (2022). Chitosan magnetic graphene grafted polyaniline doped with cobalt oxide for removal of arsenic(V) from water. *Environmental Research, 207*, Article 112209. https://doi.org/10.1016/J.ENVRES.2021.112209

Ganguly, S., Das, P., Itzhaki, E., Hadad, E., Gedanken, A., & Margel, S. (2020). Microwave-synthesized polysaccharide-derived carbon dots as therapeutic cargoes and toughening agents for elastomeric gels. *ACS Applied Materials and Interfaces, 12*(46), 51940–51951. https://doi.org/10.1021/acsami.0c14527

Gerkins, C., Hajjar, R., Oliero, M., & Santos, M. M. (2022). Assessment of gut barrier integrity in mice using fluorescein-isothiocyanate-labeled dextran. *Journal of Visualized Experiments, 2022*(189), Article e64710. https://doi.org/10.3791/64710

Gilley, A. D., Arca, H. C., Nichols, B. L. B., Mosquera-Giraldo, L. I., Taylor, L. S., Edgar, K. J., & Neilson, A. P. (2017). Novel cellulose-based amorphous solid dispersions enhance quercetin solution concentrations in vitro. *Carbohydrate Polymers, 157*, 86–93. https://doi.org/10.1016/j.carbpol.2016.09.067

Glabe, C. G., Harty, P. K., & Rosen, S. D. (1983). Preparation and properties of fluorescent polysaccharides. *Analytical Biochemistry, 130*(2), 287–294. https://doi.org/10.1016/0003-2697(83)90590-0

Gonzalez, N. N., Cerri, G., Molpeceres, J., Cossu, M., Rassu, G., Giunchedi, P., & Gavini, E. (2022). Surfactant-free chitosan/cellulose acetate phthalate nanoparticles: An attempt to solve the needs of captopril administration in paediatrics. *Pharmaceuticals, 15*(6). https://doi.org/10.3390/ph15060662

Guo, J., Tang, J., Wang, J., Mao, S., Li, H., Wang, Y., … Belfiore, L. A. (2018). Europium (III)-induced water-soluble nano-aggregates of hyaluronic acid and chitosan: Structure and fluorescence. *MRS Communications, 8*(3), 1224–1229. https://doi.org/10.1557/mrc.2018.107

Horrocks, A. R., Kandola, B. K., Davies, P. J., Zhang, S., & Padbury, S. A. (2005). Developments in flame retardant textiles – A review. *Polymer Degradation and Stability, 88*(1), 3–12. https://doi.org/10.1016/J.POLYMDEGRADSTAB.2003.10.024

Hu, S., Wei, Z., Chang, Q., Trinchi, A., & Yang, J. (2016). A facile and green method towards coal-based fluorescent carbon dots with photocatalytic activity. *Applied Surface Science, 378*, 402–407. https://doi.org/10.1016/J.APSUSC.2016.04.038

Huang, Y., Dan, N., Dan, W., & Zhao, W. (2019). *Reinforcement of Polycaprolactone/chitosan with nanoclay and controlled release of curcumin for wound dressing*. https://doi.org/10.1021/acsomega.9b02217

Ilevbare, G. A., Liu, H., Edgar, K. J., & Taylor, L. S. (2013). Impact of polymers on crystal growth rate of structurally diverse compounds from aqueous solution. *Molecular Pharmaceutics, 10*(6), 2381–2393. https://doi.org/10.1021/mp400029v

Jaiswal, A., Sankar Ghosh, S., & Chattopadhyay, A. (2011). One step synthesis of C-dots by microwave mediated caramelization of poly(ethylene glycol). *Chemical Communications, 48*(3), 407–409. https://doi.org/10.1039/C1CC15988G

Jana, J., Ganguly, M., Das, B., Dhara, S., Negishi, Y., & Pal, T. (2016). One pot synthesis of intriguing fluorescent carbon dots for sensing and live cell imaging. *Talanta, 150*, 253–264. https://doi.org/10.1016/J.TALANTA.2015.12.047

Janda, J., & Work, E. (1971). *A colorimetric estimation of lipopolysaccharides* (p. 16).

Kaneo, Y., Tanaka, T., Nakano, T., & Yamaguchi, Y. (2001). Evidence for receptor-mediated hepatic uptake of pullulan in rats. *Journal of Controlled Release, 70*(3), 365–373. https://doi.org/10.1016/S0168-3659(00)00368-0

Karimi Jabali, M., Allafchian, A. R., Jalali, S. A. H., Shakeripour, H., Mohammadinezhad, R., & Rahmani, F. (2022). Design of a pDNA nanocarrier with ascorbic acid modified chitosan coated on superparamagnetic iron oxide nanoparticles for gene delivery. *Colloids and Surfaces A: Physicochemical and Engineering Aspects, 632*, Article 127743. https://doi.org/10.1016/j.colsurfa.2021.127743

Kohn, J., & Wilchek, M. (1978). A colorimetric method for monitoring activation of sepharose by cyanogen bromide. *Biochemical and Biophysical Research Communications, 84*(1), 7–14. https://doi.org/10.1016/0006-291X(78)90255-3

Kondaveeti, S., Chejara, D. R., & Siddhanta, A. K. (2013). A facile one-pot synthesis of a fluorescent agarose-O-naphthylacetyl adduct with slow release properties. *Carbohydrate Polymers, 98*(1), 589–595. https://doi.org/10.1016/j.carbpol.2013.06.046

Kondaveeti, S., Mehta, G. K., & Siddhanta, A. K. (2014). Modification of agarose: 6-Aminoagarose mediated syntheses of fluorogenic pyridine carboxylic acid amides. *Carbohydrate Polymers, 106*(1), 365–373. https://doi.org/10.1016/j.carbpol.2014.02.051

Kong, W., Liu, R., Li, H., Liu, J., Huang, H., Liu, Y., & Kang, Z. (2014). High-bright fluorescent carbon dots and their application in selective nucleoli staining. *Journal of Materials Chemistry B, 2*(31), 5077–5082. https://doi.org/10.1039/C4TB00579A

Lai, X., Han, Y., Zhang, J., Zhang, J., Lin, W., Liu, Z., & Wang, L. (2021). Peroxidase-like platinum clusters synthesized by ganoderma lucidum polysaccharide for sensitively colorimetric detection of dopamine. *Molecules, 26*(9). https://doi.org/10.3390/molecules26092738

Lakowicz, J. R. (2006a). Principles of fluorescence spectroscopy, 3rd principles of fluorescence spectroscopy, springer, New York, USA, 3rd edn, 2006. In *Principles of fluorescence spectroscopy, Springer, New York, USA, 3rd edn, 2006*. https://doi.org/10.1007/978-0-387-46312-4

Lakowicz, J. R. (2006b). Principles of fluorescence spectroscopy. In *Principles of fluorescence spectroscopy*. https://doi.org/10.1007/978-0-387-46312-4

Lawrence, J. R., Neu, T. R., & Swerhone, G. D. W. (1998). Application of multiple parameter imaging for the quantification of algal, bacterial and exopolymer components of microbial biofilms. *Journal of Microbiological Methods, 32*(3), 253–261. https://doi.org/10.1016/S0167-7012(98)00027-X

Lencer, W. I., Weyer, P., Verkman, A. S., Ausiello, D. A., & Brown, D. (1990). FITC-dextran as a probe for endosome function and localization in kidney. *American Journal of Physiology - Cell Physiology, 258*(2 27-2). https://doi.org/10.1152/ajpcell.1990.258.2.c309

Li, B., Konecke, S., Harich, K., Wegiel, L., Taylor, L. S., & Edgar, K. J. (2013). Solid dispersion of quercetin in cellulose derivative matrices influences both solubility and stability. *Carbohydrate Polymers, 92*(2), 2033–2040. https://doi.org/10.1016/j.carbpol.2012.11.073

Li, C., Tang, Q., Wei, H., Liu, J., Wang, Q., Wang, Y., … Tang, J. (2022). Smart wearable fluorescence sensing of bacterial pathogens and toxic contaminants by Eu3+-induced sodium alginate/ag nanoparticle aggregates. *ACS Applied Nano Materials, 5*(6), 8393–8403. https://doi.org/10.1021/acsanm.2c01525

Li, F., Liu, Y. T., Li, Z. M., Li, Q., Liu, X. Y., & Cui, H. (2020). Cu(II)-regulated on-site assembly of highly chemiluminescent multifunctionalized carbon nanotubes for inorganic pyrophosphatase activity determination. *ACS Applied Materials & Interfaces, 12*(2), 2903–2909. https://doi.org/10.1021/acsami.9b20259

Li, L., Jia, C., Wang, F., Fan, H., Jiao, W., & Shao, Z. (2018). Facile synthesis of magnetic fluorescent nanoparticles: Adsorption and selective detection of Hg(II) in water. *Journal of Materials Chemistry C, 6*(9), 2360–2369. https://doi.org/10.1039/c7tc05564a

Li, L., Jia, C., Wang, F., Fan, H., Jiao, W., & Shao, Z. (2018). Facile synthesis of magnetic fluorescent nanoparticles: Adsorption and selective detection of Hg(II) in water †. *2360 |. Journal of Materials Chemistry C, 6*, 2360. https://doi.org/10.1039/c7tc05564a

Liao, J., Cheng, Z., & Zhou, L. (2016). Nitrogen-doping enhanced fluorescent carbon dots: Green synthesis and their applications for bioimaging and label-free detection of Au 3+ ions. *ACS Sustainable Chemistry & Engineering, 4*, 3061. https://doi.org/10.1021/acssuschemeng.6b00018

Liu, H., Taylor, L. S., & Edgar, K. J. (2015). The role of polymers in oral bioavailability enhancement; A review. *Polymer, 77*, 399–415. https://doi.org/10.1016/j.polymer.2015.09.026

Liu, H., Yin, Y., Zhou, J., Yang, H., Guo, L., Peng, F., & Qi, H. (2022). Fabrication of durable fluorescent and hydrophobic cotton fabrics by multiple surface modifications. *Industrial Crops and Products, 175*(6), 2000496. https://doi.org/10.1016/j.indcrop.2021.114238

Liu, S., Zhao, N., Cheng, Z., & Liu, H. (2015). Amino-functionalized green fluorescent carbon dots as surface energy transfer biosensors for hyaluronidase †. *7*, 6836. https://doi.org/10.1039/c5nr00070j

Lukomska, J., Rzeska, A., Malicka, J., & Wiczk, W. X. (2001). Influence of a substituent on amide nitrogen atom on fluorescence efficiency quenching of Tyr(Me) by amide group. *Journal of Photochemistry and Photobiology A: Chemistry, 143*(2–3), 135–139. https://doi.org/10.1016/S1010-6030(01)00521-4

Malzahn, K., Marsico, F., Koynov, K., Landfester, K., Weiss, C. K., & Wurm, F. R. (2014). Selective interfacial olefin cross metathesis for the preparation of hollow nanocapsules. *ACS Macro Letters, 3*(1), 40–43. https://doi.org/10.1021/MZ400578E/SUPPL_FILE/MZ400578E_SI_001.PDF

Mansur, A. A. P., Mansur, H. S., Soriano-Araujo, A., & Lobato, Z. I. P. (2014). Fluorescent nanohybrids based on quantum dot-chitosan-antibody as potential cancer biomarkers. *ACS Applied Materials & Interfaces, 6*(14), 11403–11412. https://doi.org/10.1021/am5019989

Martinez, M. N., & Amidon, G. L. (2002). A mechanistic approach to understanding the factors affecting drug absorption: A review of fundamentals. *Journal of Clinical Pharmacology, 42*(6), 620–643. https://doi.org/10.1177/00970002042006005

Mary, S. K., Koshy, R. R., Arunima, R., Thomas, S., & Pothen, L. A. (2022). A review of recent advances in starch-based materials: Bionanocomposites, pH sensitive films, aerogels and carbon dots. *Carbohydrate Polymer Technologies and Applications, 3*. https://doi.org/10.1016/J.CARPTA.2022.100190

Meng, X., & Edgar, K. J. (2015). Synthesis of amide-functionalized cellulose esters by olefin cross-metathesis. *Carbohydrate Polymers, 132*, 565–573. https://doi.org/10.1016/j.carbpol.2015.06.052

Meng, X., Matson, J. B., & Edgar, K. J. (2014a). Olefin cross-metathesis, a mild, modular approach to functionalized cellulose esters. *Polymer Chemistry, 5*(24), 7021–7033. https://doi.org/10.1039/c4py01102c

Meng, X., Matson, J. B., & Edgar, K. J. (2014b). Olefin cross-metathesis as a source of polysaccharide derivatives: Cellulose ω-carboxyalkanoates. *Biomacromolecules, 15*(1), 177–187. https://doi.org/10.1021/bm401447v

Meng, X., Tian, F., Yang, J., He, C. N., Xing, N., & Li, F. (2010). Chitosan and alginate polyelectrolyte complex membranes and their properties for wound dressing application. *Journal of Materials Science: Materials in Medicine, 21*(5), 1751–1759. https://doi.org/10.1007/s10856-010-3996-6

Messai, I., Lamalle, D., Munier, S., Verrier, B., Ataman-Önal, Y., & Delair, T. (2005). Poly (D,L-lactic acid) and chitosan complexes: Interactions with plasmid DNA. *Colloids and Surfaces A: Physicochemical and Engineering Aspects, 255*(1–3), 65–72. https://doi.org/10.1016/j.colsurfa.2004.12.023

Michael, T., & Smith, C. M. (1995). Lectins probe molecular films in biofouling: Characterization of early films on non-living and living surfaces. *Marine Ecology Progress Series, 119*(1–3), 229–236. https://doi.org/10.3354/MEPS119229

Mosquera-Giraldo, L. I., H. Borca, C., S. Parker, A., Dong, Y., J. Edgar, K., P. Beaudoin, S., … S. Taylor, L. (2018). Crystallization inhibition properties of cellulose esters and ethers for a group of chemically diverse drugs: experimental and computational insight. *Biomacromolecules, 19*(12), 4593–4606. https://doi.org/10.1021/acs.biomac.8b01280

Mrozek, J., Banecki, B., Karolczak, J., & Wiczk, W. (2005). Influence of the separation of the charged groups and aromatic ring on interaction of tyrosine and phenylalanine analogues and derivatives with β-cyclodextrin. *Biophysical Chemistry, 116*(3), 237–250. https://doi.org/10.1016/J.BPC.2005.04.011

Natarajan, R., Northrop, N., & Yamamoto, B. (2017). Fluorescein isothiocyanate (FITC)-dextran extravasation as a measure of blood-brain barrier permeability. *Current Protocols in Neuroscience, 79*(1), 9.58.1–9.58.15. https://doi.org/10.1002/CPNS.25

Natarajan, S., Jayaraj, J., & Prazeres, D. M. F. (2021). A cellulose paper-based fluorescent lateral flow immunoassay for the quantitative detection of cardiac troponin I. *Biosensors, 11*(2), 49. https://doi.org/10.3390/BIOS11020049

Nawaz, H., Zhang, X., Chen, S., You, T., & Xu, F. (2021). Recent studies on cellulose-based fluorescent smart materials and their applications: A comprehensive review. *Carbohydrate Polymers, 267*. https://doi.org/10.1016/J.CARBPOL.2021.118135

Neu, T. R. (2000). In situ cell and glycoconjugate distribution in river snow studied by confocal laser scanning microscopy. *Aquatic Microbial Ecology, 21*(1), 85–95. https://doi.org/10.3354/ame021085

Novo, D. C., Gao, C., Qi, Q., Mosquera-Giraldo, L. I., Spiering, G. A., Moore, R. B., … Edgar, K. J. (2022). Designing synergistic crystallization inhibitors: Bile salt derivatives of cellulose with enhanced hydrophilicity. *Carbohydrate Polymers, 292*, Article 119680. https://doi.org/10.1016/j.carbpol.2022.119680

Nowak, N., Grzebieniarz, W., Gohar, K., Khachatryan, K., Konieczna-Molenda, A., Krzan, M., … Pl, A. K. (2021). *Synthesis of silver and gold nanoparticles in sodium alginate matrix enriched with graphene oxide and investigation of properties of the obtained thin films*. https://doi.org/10.3390/app11093857

Nualnoi, T., Kirosingh, A., Pandit, S. G., Thorkildson, P., Brett, P. J., Burtnick, M. N., & AuCoin, D. P. (2016). In vivo distribution and clearance of purified capsular polysaccharide from Burkholderia pseudomallei in a murine model. *PLoS Neglected Tropical Diseases, 10*(12), Article e0005217. https://doi.org/10.1371/journal.pntd.0005217

Ohtake, K., Natsume, H., Ueda, H., & Morimoto, Y. (2002). Analysis of transient and reversible effects of poly-L-arginine on the in vivo nasal absorption of FITC-dextran in rats. *Journal of Controlled Release, 82*(2–3), 263–275. https://doi.org/10.1016/S0168-3659(02)00128-1

Oza, M. D., Meena, R., Prasad, K., Paul, P., & Siddhanta, A. K. (2010). Functional modification of agarose: A facile synthesis of a fluorescent agarose–guanine derivative. *Carbohydrate Polymers, 81*(4), 878–884. https://doi.org/10.1016/J.CARBPOL.2010.03.062

Oza, M. D., Meena, R., & Siddhanta, A. K. (2012). Facile synthesis of fluorescent polysaccharides: Cytosine grafted agarose and κ-carrageenan. *Carbohydrate Polymers, 87*(3), 1971–1979. https://doi.org/10.1016/j.carbpol.2011.10.004

Oza, M. D., Prasad, K., & Siddhanta, A. K. (2012). One-pot synthesis of fluorescent polysaccharides: Adenine grafted agarose and carrageenan. *Carbohydrate Research, 357*, 23–31. https://doi.org/10.1016/j.carres.2012.05.016

Panda, A., Sharma, P. K., McCann, T., Bloomekatz, J., Repka, M. A., & Murthy, S. N. (2022). Fabrication and development of controlled release PLGA microneedles for macromolecular delivery using FITC-dextran as model molecule. *Journal of Drug Delivery Science and Technology, 68*, Article 102712. https://doi.org/10.1016/j.jddst.2021.102712

Peng, F., Liu, H., Xiao, D., Guo, L., Yue, F., Würfe, H., Heinze, T., & Qi, H. (2022). Green fabrication of high strength, transparent cellulose-based films with durable fluorescence and UV-blocking performance. *Journal of Materials Chemistry A, 10*(14), 7811–7817. https://doi.org/10.1039/d2ta00817c

Pereira, F. A. R., Sousa, K. S., Cavalcanti, G. R. S., França, D. B., Queiroga, L. N. F., Santos, I. M. G., … Jaber, M. (2017). Green biosorbents based on chitosan-montmorillonite beads for anionic dye removal. *Journal of Environmental Chemical Engineering, 5*(4), 3309–3318. https://doi.org/10.1016/j.jece.2017.06.032

Pereira, J. M. (2013). Synthesis of new pullulan derivatives for drug delivery synthesis of new pullulan derivatives for drug delivery. http://hdl.handle.net/10919/23884.

Perreux, L., Loupy, A., & Volatron, F. (2002). Solvent-free preparation of amides from acids and primary amines under microwave irradiation. *Tetrahedron, 58*(11), 2155–2162. https://doi.org/10.1016/S0040-4020(02)00085-6

Pramod, P. S., Takamura, K., Chaphekar, S., Balasubramanian, N., & Jayakannan, M. (2012). Dextran vesicular carriers for dual encapsulation of hydrophilic and hydrophobic molecules and delivery into cells. *13*, 47. https://doi.org/10.1021/bm301583s

Reichardt, C. (1994). Solvatochromic dyes as solvent polarity indicators. *Chemical Reviews, 94*(8), 2319–2358. https://doi.org/10.1021/cr00032a005

Richter, A. P., Brown, J. S., Bharti, B., Wang, A., Gangwal, S., Houck, K., … Velev, O. D. (2015). An environmentally benign antimicrobial nanoparticle based on a silver-infused lignin core. *Nature Nanotechnology, 10*(9), 817–823. https://doi.org/10.1038/nnano.2015.141

Salgado, C. L., Mansur, A. A. P., Mansur, H. S., & Monteiro, F. J. M. (2021). Bioengineered fluorescent nanoprobe conjugates for tracking human bone cells: In vitro biocompatibility analysis. *Materials, 14*(16). https://doi.org/10.3390/ma14164422

Samal, S. K., Dash, M., Van Vlierberghe, S., Kaplan, D. L., Chiellini, E., van Blitterswijk, C., … Dubruel, P. (2012). Cationic polymers and their therapeutic potential. *Chemical Society Reviews, 41*(21), 7147–7194. https://doi.org/10.1039/c2cs35094g

Sato, K., & Anzai, J. I. (2006). Fluorometric determination of sugars using fluorescein-labeled concanavalin A-glycogen conjugates. *Analytical and Bioanalytical Chemistry, 384*(6), 1297–1301. https://doi.org/10.1007/s00216-005-0279-z

Shahadat, M., Jha, A., Shahid-ul-Islam, Adnan, R., Ali, S. W., Ismail, I. M. I., … Ahammad, S. Z. (2022). Recent advances in chitosan-polyaniline based nanocomposites for environmental applications: A review. *Polymer, 254*. https://doi.org/10.1016/J.POLYMER.2022.124975

Siddhanta, A. K., Sanandiya, N. D., Chejara, D. R., & Kondaveeti, S. (2015). Functional modification mediated value addition of seaweed polysaccharides – A perspective. *RSC Advances, 5*(73), 59226–59239. https://doi.org/10.1039/c5ra09027j

Song, Y., Li, Y., Liu, Z., Liu, L., Wang, X., Su, X., & Ma, Q. (2014). A novel ultrasensitive carboxymethyl chitosan-quantum dot-based fluorescence "turn on-off" nanosensor for lysozyme detection. *Biosensors and Bioelectronics, 61*, 9–13. https://doi.org/10.1016/J.BIOS.2014.04.036

Sun, M., Wang, X., Cheng, X., He, L., Yan, G., & Tang, R. (2018). TPGS-functionalized and ortho ester-crosslinked dextran nanogels for enhanced cytotoxicity on multidrug resistant tumor cells. *Carbohydrate Polymers, 198*, 142–154. https://doi.org/10.1016/J.CARBPOL.2018.06.079

Teja, S. B., Patil, S. P., Shete, G., Patel, S., & Bansal, A. K. (2016). Drug-excipient behavior in polymeric amorphous solid dispersions. *Journal of Excipients and Food Chemicals, 4*(3).

Virmani, M., Deshpande, N. U., Pathan, S., & Jayakannan, M. (2021). Self-reporting polysaccharide polymersome for doxorubicin and cisplatin delivery to live cancer cells. *2*, 181–193. https://doi.org/10.1021/acspolymersau.1c00042

Waggoner, A. (1995). [15] Covalent labeling of proteins and nucleic acids with fluorophores. *Methods in Enzymology, 246*(C), 362–373. https://doi.org/10.1016/0076-6879(95)46017-9

Wan Ngah, W. S., Teong, L. C., & Hanafiah, M. A. K. M. (2011). Adsorption of dyes and heavy metal ions by chitosan composites: A review. In , *Vol. 83, Issue 4. Carbohydrate polymers* (pp. 1446–1456). https://doi.org/10.1016/j.carbpol.2010.11.004

Wang, C., Wang, F., Zhang, J., Liu, L., Xu, G., & Dou, H. (2020). Fluorescent polysaccharide nanogels for the detection of tumor heterogeneity in drug-surviving cancer cells. *Advanced Biosystems, 4*(2), 1–10. https://doi.org/10.1002/adbi.201900213

Wang, R., Sun, S., Wang, B., Mao, Z., Xu, H., Feng, X., & Sui, X. (2021). Robust fabrication of fluorescent cellulosic materials via Hantzsch reaction. *Macromolecular Rapid Communications, 42*(6). https://doi.org/10.1002/marc.202000496

Wang Yu Liu Joo-Hwa Tay, Z.-W. (2005). APPLIED MICROBIAL AND CELL PHYSIOLOGY distribution of EPS and cell surface hydrophobicity in aerobic granules. *Applied Microbiology and Biotechnology, 69*, 469–473. https://doi.org/10.1007/s00253-005-1991-5

Wani, A. A., Khan, A. M., Manea, Y. K., Salem, M. A. S., & Shahadat, M. (2021). Selective adsorption and ultrafast fluorescent detection of Cr(VI) in wastewater using neodymium doped polyaniline supported layered double hydroxide nanocomposite. *Journal of Hazardous Materials, 416*. https://doi.org/10.1016/j.jhazmat.2021.125754

Webber, S. E. (1999). Fluorescence of polymers: A probe of polymer assemblies. *Macromolecular Symposia, 143*, 359–370. https://doi.org/10.1002/masy.19991430126

Weecharangsan, W., Opanasopit, P., Ngawhirunpat, T., Apirakaramwong, A., Rojanarata, T., Ruktanonchai, U., & Lee, R. J. (2008). Evaluation of chitosan salts as non-viral gene vectors in CHO-K1 cells. *International Journal of Pharmaceutics, 348*(1–2), 161–168. https://doi.org/10.1016/j.ijpharm.2007.07.011

Wempe, M. F., Wright, C., Little, J. L., Lightner, J. W., Large, S. E., Caflisch, G. B., … Edgar, K. J. (2009). Inhibiting efflux with novel non-ionic surfactants: Rational design based on vitamin E TPGS. *International Journal of Pharmaceutics, 370*(1–2), 93–102. https://doi.org/10.1016/j.ijpharm.2008.11.021

Weng, C. I., Chang, H. T., Lin, C. H., Shen, Y. W., Unnikrishnan, B., Li, Y. J., & Huang, C. C. (2015). One-step synthesis of biofunctional carbon quantum dots for bacterial labeling. *Biosensors and Bioelectronics, 68*, 1–6. https://doi.org/10.1016/J.BIOS.2014.12.028

Wiederschain, G. Y. (2011). The molecular probes handbook. A guide to fluorescent probes and labeling technologies. *Biochemistry (Moscow), 76*(11), 1276. https://doi.org/10.1134/s0006297911110101

Wilson, V., Lou, X., Osterling, D. J., Stolarik, D. F., Jenkins, G., Gao, W., … Taylor, L. S. (2018). Relationship between amorphous solid dispersion in vivo absorption and in vitro dissolution: Phase behavior during dissolution, speciation, and membrane mass transport. *Journal of Controlled Release: Official Journal of the Controlled Release Society, 292*, 172–182. https://doi.org/10.1016/j.jconrel.2018.11.003

Wilson, V. R., Lou, X., Osterling, D. J., Stolarik, D. F., Jenkins, G. J., Nichols, B. L. B., … Taylor, L. S. (2020). Amorphous solid dispersions of enzalutamide and novel polysaccharide derivatives: Investigation of relationships between polymer structure and performance. *Scientific Reports, 10*(1), 18535. https://doi.org/10.1038/s41598-020-75077-7

Wu, W., Yao, W., Wang, X., Xie, C., Zhang, J., & Jiang, X. (2015). Bioreducible heparin-based nanogel drug delivery system. *Biomaterials, 39*, 260–268. https://doi.org/10.1016/j.biomaterials.2014.11.005

Yu, J., Xu, C., Tian, Z., Lin, Y., & Shi, Z. (2016). Facilely synthesized N-doped carbon quantum dots with high fluorescent yield for sensing Fe 3+. *New Journal of Chemistry, 40*, 2083. https://doi.org/10.1039/c5nj03252k

Zhang, Z., He, Z., Weng, T., Tong, L., Liu, Y., Chen, Y., & Zhou, M. (2023). Fabrication of stable solid fluorescent starch materials based on Hantzsch reaction. *Carbohydrate Polymers, 314*, Article 120811. https://doi.org/10.1016/j.carbpol.2023.120811

Zheng, Z., Pan, X., Xu, J., Wu, Z., Zhang, Y., & Wang, K. (2020). Advances in tracking of polysaccharides in vivo: Labeling strategies, potential factors and applications based on pharmacokinetic characteristics. *International Journal of Biological Macromolecules, 163*, 1403–1420. https://doi.org/10.1016/j.ijbiomac.2020.07.210

Zheng, Z.-M., Zhang, Y., Zhang, Q.-L., Luo, L., Pan, X.-L., & Wang, K.-P. (2022). Polysaccharide radioisotopic labeling and its application in pharmacokinetics study in vivo. *Chinese Pharmaceutical Journal, 57*(8), 599–604. https://doi.org/10.11669/cpj.2022.08.003

Zhou, J., Li, N., Liu, P., Liu, Z., Gao, L., & Jiao, T. (2022). Preparation of fluorescently labeled chitosan-quercetin drug-loaded nanoparticles with excellent antibacterial properties. In *, Vol. 13, Issue 3. Journal of functional biomaterials*. https://doi.org/10.3390/jfb13030141

Zhou, J. W., Zou, X. M., Song, S. H., & Chen, G. H. (2018). Quantum dots applied to methodology on detection of pesticide and veterinary drug residues. In *Journal of agricultural and food chemistry (Vol. 66, issue 6, pp. 1307–1319). American Chemical Society*. https://doi.org/10.1021/acs.jafc.7b05119